

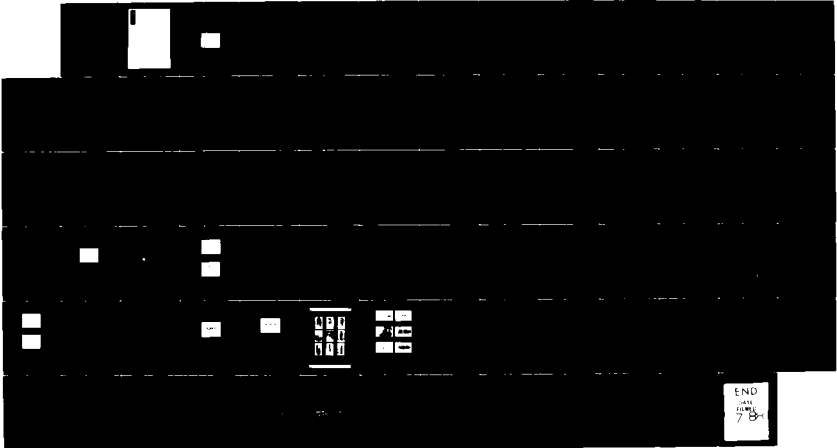
AD-A193 360

BASIC MECHANISMS OF DIESEL LUBRICATION CORRELATION OF  
BENCH AND ENGINE TESTS (U) CAMBRIDGE UNIV (ENGLAND)  
A F ALLISTON-GREINER ET AL. AUG 87 DAJ45-86-C-0007  
F/G 11/8

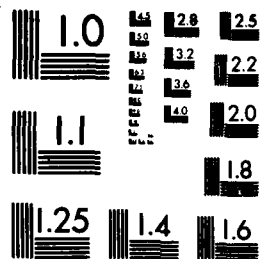
1/1

UNCLASSIFIED

NL



END  
75



MICROCOPY RESOLUTION TEST CHART  
NATIONAL BUREAU OF STANDARDS 1963 A

AD-A193 360

ERRATA

Figures 11, 13, 15-17, 19, 20, 36-38  
horizontal time axis not marked.  
The scale is one square = 5 minutes.

Figure 14 time axis, one square = 30 seconds.

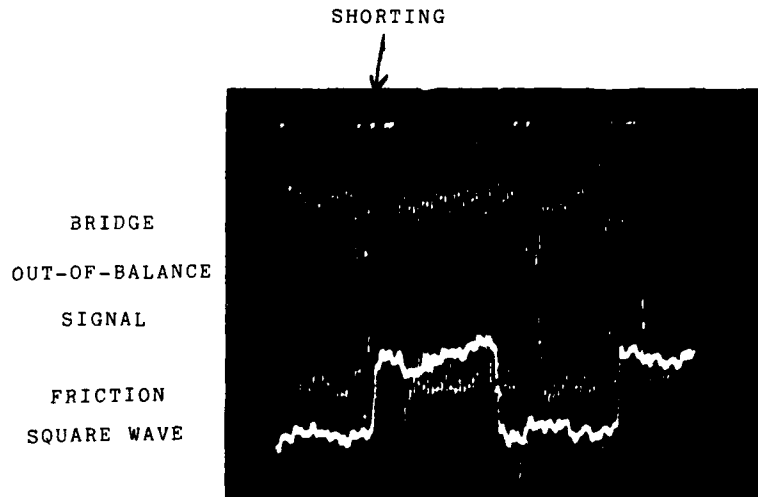


FIGURE 6

FRICTION AND CAPACITANCE TRACES FROM  
OSCILLOSCOPE SHOWING SHORTING OF  
CAPACITANCE DUE TO METAL-METAL CONTACT

**BASIC MECHANISMS OF DIESEL LUBRICATION  
CORRELATION OF BENCH AND ENGINE TESTS**

Contract No. DAJA 45 36 C0007

**First Annual Report**

**1 SUMMARY**

- 1 A newly designed reciprocating ball-on-flat apparatus is described.
- 2 Reaction film formation by commercially available ZDDP additives were observed and their thicknesses measured by capacitance during the rubbing process. The film behaviour is related to its composition and the thermal stability and reactivity of the additives.
- 3 Preliminary observation is made of the running-in process with cast-iron cylinder liners.
- 4 The programme of work proposed for the coming year is detailed in the Appendix.

Accession For	
NTIS CRA&I	<input checked="" type="checkbox"/>
DTIC TAB	<input type="checkbox"/>
Unannounced	<input type="checkbox"/>
Justification	
By <i>Smith</i>	
Distribution /	
Availability Codes	
Dist	Avail and/or Special
<i>A-1</i>	



## CONTENTS

1	SUMMARY
2	OBJECT
3	INTRODUCTION
4	RECIPROCATING RIG
	4.1 Apparatus
	4.2 Electrical contact resistance
	4.3 Contact capacitance
	4.4 Load and friction force
	4.5 Heating and temperature measurement
	4.6 Cleaning
	4.7 Film thickness measurement
	4.8 Dielectric constant
5	REACTION FILMS FORMED BY ZDDP ON STEEL AND CAST IRON
	5.1 Film formation
	5.2 Wear reduction
	5.3 Variation of film thickness with load
	5.4 Variation of film thickness with temperature
	5.5 Shear properties of the reaction films
6	DISCUSSION
	6.1 Film formation and wear reduction
	6.2 Film properties
	6.3 Effect of temperature
7	CONCLUSIONS
8	APPENDIX - Programme for Year 2
9	REFERENCES

2      **OBJECT**

The final aim of this project is to produce a method of assessing cylinder liner quality in a laboratory test machine, to reduce the amount of full-scale testing. The possibility of devising a much shorter, but equally effective running-in procedure should also follow.

In order to do this effectively, a study has to be made of the type of lubrication encountered in the cylinder liner/piston ring contact. This report seeks to expand the understanding of the role of the anti-wear additive zinc dialkyldithiophosphate (ZDDP) from observations of the action of the additive in the contact forming a reaction film. Measurements of the film thickness are also part of the research.

This report outlines the reasons for using the reciprocating ball-on-flat rig developed for this work and the measuring techniques. The discussion brings out the salient features of the work and relates them to the lubrication of cylinder liner contacts.

### 3 INTRODUCTION

There have been many observations of reactions between oils containing zinc dialkyldithiophosphate and steel, forming 'varnish-like' films on the metal surface [1-4]. Much about their mode of formation in a contact remains obscure. Monitoring the electrical contact resistance during running is the normal method of detecting their formation [5]. The electrical contact resistance, however, can only give an indication of the effectiveness of the film in reducing solid-solid contact, and cannot give a measurement of film thickness [6]. There has been an attempt to make a quantitative relationship between the degree of asperity interaction and the nominal elastohydrodynamic film thickness for a disc machine contact [7]. This relies on calculating the ehl film thickness.

Measurement of the thickness of reaction films therefore poses a problem. Much work has been done on films already formed on surfaces, either after running in a contact or by dipping a steel plate or 'coupon' in heated oil. The thickness of the resultant film can be determined optically, by scratching the film and observing the shadow cast by a light. Scanning electron microscopy coupled with a chemical analysis system (e.g. Auger Spectroscopy) is also used. Films between 60 nm and 2  $\mu\text{m}$  [8-10] have been reported. The objections to this 'static' study is that the surfaces have to be cleaned before observation, which probably removes some, unknown, amount of loosely bound material. Also the method of film formation with a dipped coupon is different from its formation in a rubbing contact, since the rubbed surfaces take part in the reaction (see below). This is an important but often overlooked consideration.

It has been found that even under conditions of nominally pure rolling, the film in the wear track is far thicker than on the surrounding surfaces [11]. It is believed that the thick film is due to the rubbing process which removes protective oxides and exposes active metal surface,

which in some way promotes film formation. Usually the rubbing metals are polyvalent such as iron, chromium, etc., which are good catalysts. It is most desirable therefore that any study of the reaction film should be of a film resulting from a rubbing process with carefully controlled contact temperatures (see below). Dipping surfaces into heated oil is much less satisfactory as the resultant film was not formed during the frictional process.

These varnish films are formed by chemical reaction, and so presumably are very temperature sensitive. Hence the temperatures at which the film is formed is of considerable importance and should be known accurately. Furthermore it is well known in accelerated oxidation tests that the reaction mechanism changes with temperature. Hence to study the action of E.P. additives correctly the contact temperatures must be identical in test rig and engine. The problem in most sliding contact bench experiments is that the contact temperature is not known accurately. This is because the contact temperature is made up of a 'bulk' component together with a transient component due to frictional heating. A thermocouple placed near the contact, or embedded in the surface does not pick up this flash temperature, which can be very appreciable [12, 13]. Furthermore where the film is formed in a friction device running at slow speeds to enable the contact temperature to be accurately determined, the rate of contact repetition is wrong. This is discussed further below.

The first study of the formation and simultaneous measurement of a reaction film thickness was using an optical ehl device [11]. Temperatures up to 99°C were achieved, and a very reactive oil was used. The optical method demands a semi-reflecting layer on a glass plate, and a very highly polished metal ball, so that the friction system was rather unusual, but the results were of great interest. Next films were observed by a capacitance method in a disc machine, running with a bulk oil temperature of 25°C

[14], but unknown contact temperature. These papers reported increases in the ehl film thicknesses due to additive action of 160 nm and 600 nm. The great disadvantage of the disc machine is that the contact temperatures are difficult to determine with certainty. A variant of the optical method [15] used balls dipped in hot oil and subsequently run in the optical device. Similar results were found.

It seems, therefore, that for a realistic study of the formation of the reaction film, four conditions must be met:

- (i) The film must be formed in a rubbing contact.
- (ii) Realistic surfaces and materials must be used.
- (iii) The temperature of the contact must be known accurately.
- (iv) The lubrication conditions should be known.

Many components, and particularly the cylinder liner/piston ring contact function in the 'mixed lubrication regime' - i.e. where there is some contribution from oil viscosity and also some contribution from boundary films. The problem in these cases is sorting out the viscous from the boundary conditions. Therefore in order to make interpretation of film properties straightforward, classical hydrodynamic lubrication should be excluded, so that the lubrication conditions are known to be purely non-viscous.

All these conditions are met in the reciprocating test rig that is described in this report. In order to make measurements of film thickness, the capacitance of the ball/flat contact is to be monitored. Deductions of the film thicknesses are made from the capacitance readings. Thus the distinctive contribution of this work is that thickness measurements are made of reaction films formed by ZDDP during running under carefully controlled conditions, (especially of temperature) and at the correct repetition contact rate.

#### 4      RECIPROCATING RIG

The development of the reciprocating rig first described in [16] has been detailed in the two interim reports [17, 18]. In this section the principle of the machine is described, and then details of the component parts of the rig are given, explaining their function.

In the piston ring/cylinder liner contact (and in any repeating contact device) it is the repetition rate rather than the speed which is important when considering interactions of surface asperities. The protective film formed by additives is completely or partially removed during each contact and must be reformed before the next one: the time available for this is crucial. The rate of reformation depends on the chemical activity of the systems (metals and oil) and of course the temperature - see [19]. Therefore knowing the contact temperature is important. However, in most test devices the speed is high (giving large and unknown flash temperatures due to frictional heating) but the repetition rate is not as in the running engine. The reciprocating apparatus therefore provides a simple device, using actual engine components, of avoiding high flash temperatures (since the sliding velocity is low), but having the correct repetition rate. This means also that the contact temperature can be controlled accurately, simply by controlling the bulk temperature of the test specimens.

##### 4.1      Apparatus

The contact configuration is ball-on-flat, the ball being reciprocated by a Ling Dynamics electro-mechanical 100 W oscillator loaded against a fixed flat (see Figure 1, reproduced from the previous reports). Standard conditions were 34.5 Hz,  $\pm$  0.5 mm. The ball is a push-fit into a 0.092" diameter hypodermic tube which holds it in place on the vibrator arm (Figure

2). The hypodermic tube provides an easy method of mounting, and also of making electrical connection. Balls used in these studies have been 3/32" diameter bearing balls, and specially produced silver steel 'pins' with radiused ends (radius 4.5 mm), hardened to 450 VHN (45 R<sub>C</sub>).

The flat is held in place on the 'boat' (Figure 1) in a clamping arrangement (Figure 2). The 'boat' is prevented from moving horizontally by a strain-gauge transducer (described later). The flats were made from AISI-01 high carbon (0.9 - 1.0%) steel gauge plate, hardened to 750 VHN (60 R<sub>C</sub>) and polished with emery paper and diamond lapping to an initial finish of 0.02  $\mu$ m cla. The flat was provided with a tapped hole to facilitate electrical connection (dimensions are given in Figure 2).

By making the clamping arrangements for the ball and flat with 'tufnol' (a phenol urea plastic) and also PTFE, electrical isolation of the rig from these parts was readily achieved. This, then, allowed not only for electrical contact resistance to be measured (here isolation does not matter), but also allowed the capacitance of the contact to be measured.

#### 4.2 Electrical Contact Resistance

This is a standard technique for monitoring contact conditions in many test devices [5, 20]. Quite simply, a voltage of approximately 15 mV is applied across the contact by means of a potential divider (see Figure 3), and the contact voltage is observed on an oscilloscope. 'Zero' volts implies that all the voltage drop is across the contact, i.e. that the contact resistance is effectively 'zero' (only a few ohms). '15 mV' on the scope implies no voltage drop across the contact, and therefore a very large or 'infinite' resistance. Its exact value depends on the size of the resistance in the potential divider. In our standard case 'infinite' means  $> 10^7 \Omega$ .

Because of the way this circuit works, a contact voltage of '7.5 mV' corresponds to a contact resistance of a value equal to the resistance of the potential divider ( $R_2$ ). Generally, the contact resistance fluctuates, sometimes high and sometimes low (see Figure 4). This gives some indication (qualitative) of the degree of asperity contact [5]. By taking the average of the signal (i.e. putting the signal through a low-pass filter) a continuous record of the 'degree of asperity contact' can be recorded. This was done, and it forms one of the three traces on a chart recorder.

#### 4.3 Contact Capacitance

Capacitance measurements have been made in other friction devices, such as piston ring/cylinder liner [21] and disc/disc [14]. The advantage of this method is that it is possible to make more quantitative estimations of both the amount of asperity contact, and the thickness of the film in the contact. However, the technique does rely on there being little or no asperity contact, since any metal-metal contact shorts out the circuit.

The essential features of our measurement system are given in Figure 5, and are similar to those mentioned above [21, 22]. The ball and the flat become the two 'active' parts of the circuit, their contact capacitance becoming the 'unknown' reactance in a 4-arm bridge circuit. The rest is earthed. Balancing the capacitance with the ball/flat just out of contact gives the value of stray capacitance, which can be deducted from the experimental values. The bridge is a Wayne Kerr B224 transformer ratioarm bridge, with the voltage supplied externally by an oscillator at 2.4 kHz and an amplitude that keeps the contact voltage at about 50 mV. In this way maximum bridge sensitivity is achieved while keeping the voltage low enough to avoid electrical break-down of the film on the contact. The unknown signal is fed into the bridge, and the out-of-balance is also

displayed on a HAMEG 208 storage oscilloscope, together with the friction trace. The bridge can then be balanced at a particular point in the stroke (say mid-stroke), and variations in the capacitance across the stroke can be observed. Metal-metal contact is observed when at particular points in the stroke, the capacitance signal is seen to have a high value, or a "short" (Figure 6).

#### 4.4 Load and Friction Force

The ball is loaded against the flat by means of a 'yoke' and lever (Figure 1), the dead weights being decoupled by a spring. Loads in these experiments were usually between 0.2 kg and 1 kg, sometimes higher. The loads had to be big enough to produce a good friction signal, but not so big that a coherent film did not form. It was found that 1 kg achieved this balance best. Nominal contact pressure therefore range from  $1.5 \text{ kN/mm}^2$  to  $2.6 \text{ kN/mm}^2$  for the bearing-ball contact.

Horizontal movement of the specimen was restrained by the strain-gauge transducer. This was an aluminium block with a thin leaf section 1 mm thick, acting as a very stiff 'spring'. Strain-gauges glued to the top and bottom surfaces (to provide compensation for bending) pick up the small strains due to the friction force on the flat, and are then amplified. The signal from the amplifier is displayed on the Hameg storage oscilloscope, and also rectified and low-pass filtered to provide an average friction force for the chart-recorder. Since the motion is sinusoidal, the friction trace is a square-wave.

The strain-gauges were calibrated by applying static loads to the aluminium block. The chart-recorder trace was calibrated using a function generator.

#### 4.5 Heating and Temperature Measurement

Heating is by hot air blown into an insulated container surrounding the friction elements. The central section of the rig (that is everything on the small base-plate) is enclosed in a thermally insulated box, which is a metal-fibre sandwich. The box is split in half, and has holes for the vibrator-arm, loading lever, force-transducer, electrical connectors and for hot air to be blown into the box. Air is blown through a tube containing a resistance heater element. The air temperature is raised from supply temperature to box temperature by this process. The hot air outlet is directed to blow just underneath the "boat". The air is from a shop air-line, and a rate of 35 l/min was found suitable.

The temperature of the contact is monitored by two thermocouples. One controls a West 2050 Programmer Controller, which switches the power to the heating element with a 'bang/bang' relay. This thermocouple is kept electrically isolated from the flat by placing it in between the nylon sheets in the specimen clamp (Figure 2), so that it does not provide an earth path which would render capacitance measurement impossible. The other thermocouple is clamped against the flat, but so that the tip is not directly in the path of blown hot air. This records the contact temperature and becomes an input to the chart recorder. The thermocouples are chromel/alumel, and the recording thermocouple is fed to a digital voltage multiplier for display purposes.

The controller can be programmed to supply up to four ramps and four dwells. Typically, contact temperature is maintained at  $150^{\circ}\text{C} \pm 1^{\circ}\text{C}$ , and ramp-rates of  $5^{\circ}\text{C}/\text{min}$  and  $25^{\circ}\text{C}/\text{min}$  are used.

#### 4.6 Cleaning

Cleaning of the entire rig is important. To facilitate this, the central section is made in 18/8 stainless steel so that excess oil can be burned-off and cleaned without harm. It can therefore be thoroughly cleaned when a change of additive is made. Trace amounts of additive seem to make a big difference. The ball and flat specimens are cleaned ultrasonically first in acetone and then in pentane. They are then assembled in the rig carefully, coating them in the oil to be used in the experiment as soon as possible.

#### 4.7 Film Thickness Measurement

Mostly, capacitance readings were taken at mid-stroke, and a typical out-of-balance signal is shown in Figure 7a. The signal is nulled (Fig. 7b) giving a combined capacitance of conductance for the contact.

Film thicknesses are obtained from these capacitance readings by reference to a calibration curve (Figure 8). Calibration was done in the following way. First an unworn flat (initial finish 0.02  $\mu\text{m}$  cla) was coated with a known thickness of amorphous silicon oxide by vacuum deposition at 300°C. The thickness was measured by ellipsometry.

These coated specimens were then used as calibration film thicknesses. A ball was loaded against each flat, with the electrical connections the same as in the experiment. For ease (and because of alignment problems), the ball/flat were not loaded together in the rig, but in a jig to help this alignment. This was particularly important when using balls that had themselves been used in an experiment and had a wear-scar. Contact capacitance was measured as described earlier, and values for a range of film thicknesses and a range of wear-scar sizes were obtained. The

line in Figure 8 has been drawn for a wear scar size of 0.15 mm (diameter), which is typical of these experiments. What is surprising is that the scar size seems to have little effect on the capacitance of the contact. This could be due to misalignment of the contact, even though care was taken to load the coated specimen against the worn part of the ball. There may also be a problem that the ball was not in contact over its entire worn surface, and therefore that the 'nominal' scar size was not actually the size "seen" by the contact. This is confirmed by looking at a profile trace of a worn ball (Fig. 9). The wear scar does not produce a 'flat' on the ball, but rather reduces the curvature and roughens the surface.

The dielectric constant of the oxide film was taken to be 4.0, and that of the reaction film as 2.3 (see below). The calibration line for the reaction film was then obtained by dividing the capacitance values for a given film thickness by the ratio of the dielectric constants.

#### 4.8 Dielectric Constant

The above calibration has assumed that the dielectric constant of the reaction film is the same as that of the un-reacted oil.

It has not been possible to measure directly the dielectric properties of the reaction films formed by ZDDP because of the difficulty in producing sufficient quantities. A search of the literature reveals that measurements have been made of the dielectric constants of mineral oils containing ZDDP [23, 24] and are typically around 2.3 (i.e. the same as the base oil). The capacitance of the base oil (500 Solvent Neutral) in these studies was measured in a simple capacitance cell (Figure 10), and did not change on addition of 1% ZDDP. Thus, in the bulk, the additive does not change the dielectric properties of the oil. Again, no change in the dielectric constant was observed when a sample of oil with 1% ZDDP

was heated to about 250°C and cooled.

From current literature searches, it seems likely that the dielectric constant of the reaction film will not be greatly different from the unreacted additive. In the unlikely worst case of the dielectric constant being as large as 4.0 (c.f. a highly polar polymer) the film thickness would be larger and around twice the value calculated for  $\epsilon = 2.3$ .

## 5 REACTION FILMS FORMED BY ZDDP ON STEEL AND CAST IRON

Four different ZDDPs were used in these experiments, incorporated in a 500 Solvent Neutral (500 SN) base oil at a 1% by weight treat level. The four additive oils were designated A to D and details are given in Table 1. The essential difference between the four ZDDPs is the nature of the alkyl groups in the molecule, these are also shown in Table 1. The different alkyl groups give the ZDDPs different thermal stabilities and reactivities, although exact details are not yet available. The base oil and additives were supplied by Castrol Research Laboratories, the additives originating from Exxon and Lubrizol. No details were available about their purity.

The experimental results presented aim to demonstrate some of the features of the method of lubrication with zinc dialkyldithiophosphate additive. Results include observations of film behaviour in the rubbing contact under static and dynamic loading, with varying temperature, stroke and frequency. Additionally, and this is where this apparatus differs from other devices, measurements of film thickness are made during running and at temperatures that are comparable to a running engine. The important point is that the temperatures at which the films are formed is known.

### 5.1 Film Formation

The standard temperature for experiments was set at 150°C. This is considered to be a typical working temperature for contacts such as cam/tappet and piston ring/cylinder liner - although values much greater than this may be experienced due to transient flash and high sump temperatures. However, it should be noted that the calculated flash temperature in our experiments is only a few degrees, which means that the measured bulk temperature is effectively the contact temperature. It was also found

that 150°C was the optimum temperature for film formation, the additives readily form a reaction film that provides good surface protection.

The first observation was that film formation is rapid. This can be seen in the chart-recording of an experiment for additive C at a constant temperature of 150°C in Figure 11. The load is 1 kg, and the upper trace is the friction force, the lower trace the average electrical contact resistance. Motion was started, and the load was applied. Initially there is an 'induction time' in which no film activity is observed - in this case about 45 seconds. In these first moments of motion a high friction transient is seen, which rapidly settles down to a value just greater than  $\mu = 0.1$ . This friction transient is associated with the 'induction time' when there is no film activity and therefore little protection of the rubbing surfaces.

Subsequent to the 'induction time' the average electrical contact resistance is seen to rise rapidly from a value of almost zero to a value higher than 10 M $\Omega$  in about 30 secs to 2 minutes of rubbing (corresponding to 4000 passes or 8 m of sliding). In this time there is a small reduction in the friction force - corresponding to the observed improvement in the coherence of the reaction film. This is seen from the out-of-balance capacitance signal in this period. When the electrical contact resistance is observed to be high over the whole stroke, there is still much evidence of solid-solid contact through the film, manifested by momentary 'shorting out' of the capacitance signal. However, as motion proceeds, these asperity interactions diminish until, in most cases, they vanish. Also in this period, the value of capacitance to 'null' the trace at mid-stroke diminished, indicating that the reaction film thickness increased.

Figure 12 shows another experiment at 150°C, but this time with a variable load. After film formation at the initial load of 0.2 kg, the load was increased in steps of 0.2 kg. The averaged electrical contact

resistance trace reveals that the film was disrupted on two of these load stages (seen from the downward spikes on the trace). But, after the film was disrupted, the contact resistance once again rises rapidly to the high value - the film has re-formed.

So far these observations have been for polished steel specimens, but the same kind of effects were observed for cast-iron cylinder liner specimens. These were plateau honed 0.25% phosphorus flake graphite cast iron with a cla roughness of 1.50  $\mu\text{m}$ . These experiments show the same rapid film formation, although the time taken for appreciable asperity interaction to cease is much larger, if not infinite. A typical trace is shown in Figure 13, for oil B at 150°C and a load of 1 kg (i.e. conditions identical to those in Figure 11). A high electrical contact resistance is formed after about 2 minutes of rubbing, and solid-solid contact is reduced to almost zero within the first 10 minutes of rubbing. A second experiment is shown in Figure 14, and here the film formation takes about 3 minutes, although at the end of this time the amount of asperity interaction was still too great to make capacitance readings.

Cast iron experiments again demonstrate the resistance of the reaction film to load changes. Figure 15 is a variable load experiment at 150°C for oil B. The load is raised in 0.5 kg steps from 0.5 kg to 3 kg. At each load stage, there is a momentary loss of the high electrical contact resistance (e.c.r.), indicating a loss in film protection, but this rapidly heals giving the high e.c.r. again. The capacitance trace reveals that at each load stage solid-solid contact did not fully cease. However, some readings were obtainable, indicating film thickness values of 0.1 to 0.3  $\mu\text{m}$ , which compare favourably with values obtained for the polished steel specimens (0.1 - 1.0  $\mu\text{m}$ ). The load stage of 3 kg caused the film to show signs of failure (the high e.c.r. value is greatly reduced).

However, the additive is still effective at loads greater than 3 kg.

Figure 16 is for an experiment with a constant load of 5 kg, at 150°C with oil A. Initial film formation is after about 4 minutes of rubbing, but it then takes about 2 hours for there to be film with an appreciable reduction in solid-solid contact. This is inferred from the amount of 'fur' on the e.c.r. trace gradually reducing over this period.

Returning to the polished steel specimens, experiments have been performed with other initial temperatures from 20°C to 200°C. Two kinds of effect have been observed. The first is that at 20°C there exists what is substantially a hydrodynamic film, since at this temperature the oil is much more viscous than at 150°C, and the additive is not yet reacting. Figure 16 shows the chart recording for an experiment with a constant load of 1 kg using oil B and a 4.5 mm radius pin, with temperatures from 20 - 250°C. Photographs of the electrical contact resistance were taken from the oscilloscope (Figure 18) showing this behaviour. At 20°C there is 'lift-off' in the middle of the stroke (top trace), but no lift-off at the ends of the stroke, which is the hallmark of hydrodynamic lubrication. It should be noted that there is still a high degree of asperity interaction in these conditions. As the temperature is raised to 50°C, there is evidence of some reaction film activity, since there is a non-zero resistance at the ends of the stroke. It is far from being a coherent film, since it is noted that on this scale the resistance 'high' corresponds to only 10 k $\Omega$ .

Figure 17 also displays that at 20°C the friction coefficient,  $\mu$ , is lower than the value after a reaction film is formed. The "hydrodynamic" lubrication gives  $\mu = 0.089$ , but the pure film gives  $\mu = 0.108$ . The same effect, although less marked, was observed for the bearing ball sliding (Figure 19):  $\mu$  rises from 0.088 to 0.095. In both these experiments, a coherent film was not obtained until about 150°C.

The second effect noticed in the variable temperature experiments is slightly different. The same trend in friction force is observed,

but the hydrodynamic action is obscured. This seems to be due to some reaction film formation at the low temperature. This is shown in the results recorded in Figure 20 for a bearing ball sliding, and at the lower load of 0.2 kg. The explanation may lie in the severity of the bearing-ball contact as compared with the radiused pin. The smaller radius gives a larger contact pressure, and therefore greater local asperity pressures which may give temperature effects suitable for film formation.

During motion, the film thickness was found to be nearly constant over the entire stroke, with the main variation being at the ends of the stroke where the velocity reverses. Figure 21 is a photograph of a typical friction and bridge out-of-balance signal taken from the oscilloscope. The bridge signal is very clean, indicating that there is no asperity interaction. It has been 'nulled' at the ends of the stroke, and therefore approximately displays the film 'shape' across the stroke. It should be noted that the bridge separately balances out the capacitance and conductive parts of the 'reactance', so enabling readings of both contact capacitance and resistance.

The film shape is shown better when the signal is 'nulled' at the mid-stroke position (Figure 22). Here the almost uniform film across the stroke is readily observed. The capacitance values at the ends of the stroke are always lower than at the middle. This implies that the film thickness increases at the ends of the stroke - a rather surprising observation, since we would expect the film to be thinner where the velocity is zero. However, if the film is a solid, then this film thickness at the ends of the stroke can be attributed to a kind of "bull-dozing" effect, as the solid is sheared and pushed to the ends of the contact, and the slider 'rides-up' on the piled-up material.

What is clear is that the film does not act as classical hydrodynamics would require. The velocity varies markedly throughout the stroke, but

but the film thickness appears to be largely unchanged.

## 5.2 Wear Reduction

From visual observations of wear scar at various stages of running, it becomes apparent that most of the wear has taken place in the first 1-2 minutes. It is in this period that the reaction film is seen to form. The capacitance observations show that there is little or no solid-solid contact once the reaction film has been formed.

Simply comparing results for the additive oils with results for the base oil alone reveals that while the friction coefficient is roughly the same, the wear is very different. This is displayed in Table 2, where friction coefficients and wear scar diameters for a number of experiments are recorded. The friction coefficient is a very poor indicator of the ability of the reaction film to protect the surfaces. This same effect is shown pictorially in Table 3. The wear reducing action of the additives is very apparent: not only is the wear scar diameter reduced, but also the apparent roughness of the worn surface is lower. The profiles displayed in Table 3 were taken in a profilometer after the ball and flat had been gently rinsed in solvent to remove excess oil. This meant that most of the reaction film was still in place on the surface. The profiles are displaced by about 0.2 - 0.3  $\mu\text{m}$  on the vertical scale of the diagram to give some indication of the relative size of the apparent roughness to the reaction film thickness. At the high load of 1.0 kg, the films were about 0.3  $\mu\text{m}$  thick which was comparable to or greater than the apparent roughness of the wear scar. At the lower load of 0.2 kg, the films were about 0.6  $\mu\text{m}$  thick, and much greater than the apparent roughness of the scar.

It is, of course, this wear reducing ability of the additive that

is important in practice. A photographic record of some results for 5 kg load tests using cast-iron cylinder liner is shown in Figure 23, each picture showing the wear scar on the liner after 2 hours of rubbing. It is immediately obvious that the wear is greatly reduced from the base oil alone by addition of 1% ZDDP. The 'cross-hatch' honing marks were obliterated when the base oil was used, but are still evident after running with additive oil. Figure 24 displays photographs for experiments run for different lengths of time (5 minutes, 2 hours and 4 hours). Here it is quite striking that the wear scars are visually almost the same, indicating that most of the wear seems to have taken place in the first 5 minutes of rubbing.

### 5.3 Variation of Film Thickness with Load

At a constant temperature (100, 150 or 200°C) with a load of initially either 0.2 kg (bearing ball experiments) or 1.0 kg (for the radiused pins) motion was started. Conditions were allowed to settle down, and then a capacitance reading was taken for the mid-stroke position. The load was then either raised or lowered in steps of 0.1 kg to cover the range 0.2 - 1.0 kg. Each load was applied for 2-5 minutes before a new capacitance reading was taken. This allowed the film to establish itself under the new running conditions. This is termed the dynamic loading of the films.

At the end of the dynamic loading, motion was removed. On all but a few occasions, the film remained in the contact. It was immediately apparent that the film thickness when static was different from the dynamic readings, since the bridge out-of-balance signal changed. The film in the contact was then loaded normally and capacitance readings taken at each load stage.

Although there is some variation in the wear scar size between

each experiment, the calibration curve for deducing the film thickness was used for a typical value of wear scar diameter. The reason for this is that in calibration, the wear scar diameter (for the small sizes in these experiments) did not seem to change the capacitance value significantly. It should be noted that the wear scar on the ball is far from the 'ideal' of a flat on the ball, and is rather a roughened region where the ball contacts the flat. The variations of deduced film thickness against load are shown in Figures 25 - 28, 30 - 33.

Figures 25 - 28 are for bearing-ball experiments at 150°C, the hollow symbols correspond to the dynamic loading, and the solid symbols to the static loading. The first observation is that the film thickness decreases with load. Curves have been drawn on the figures to indicate the general trend. The curve is more nearly a straight line for the static loading, indicating that the film behaves elastically in this condition, confined in the contact. In other words, reduction in film thickness on loading is completely recovered on unloading. Another general feature is that the dynamic film thickness is on the whole lower than the static value. This clearly shows that there is little or no viscous contribution from the film, that it is a solid and is sheared in the contact. The reduction in film thickness with load during motion is probably due to an increased amount of 'smoothing' of the film, the "bull-dozing" effect mentioned in the last section.

The trends of film thickness against load (represented by the dotted lines in these figures) are compared with each other in Figures 29 and 34. There is certainly some difference between the oils in the average film thickness produced, but giving a definite order is difficult since oils B and D are so close to each other. However it does seem that oil C consistently gives the thickest films, and oil A gives the thinnest films. This is probably a reflection of the nature of the alkyl group in the ZDDP, and

will be discussed later.

Figures 30 - 33 differ in that they are for experiments with the radiused pin, not the bearing-ball. Here the same trends are observed as in the previous figures. The main difference is that the deduced film thicknesses are about half the values for the corresponding bearing-ball experiments. The range here is  $0.05 \mu\text{m} - 0.25 \mu\text{m}$ , compared with a range of  $0.1 - 0.6 \mu\text{m}$ . It is not clear whether this is a function of the calibration method with the wear scars, or whether it is a real effect of the radius of the ball. Further work needs to be done to elucidate this effect.

#### 5.4 Variation of Film Thickness with Temperature

Figures 30 - 33 display results of film thickness against load obtained at three different, constant temperatures ( $100^\circ\text{C}$ ,  $150^\circ\text{C}$  and  $200^\circ\text{C}$ ). The variation of film thickness with temperature is not very marked. There does seem to be an increase as the temperature is raised to  $200^\circ\text{C}$ , and this is seen most clearly in Figure 31. Values at  $100^\circ\text{C}$  are either comparable with those at  $150^\circ\text{C}$ , or slightly lower, which would be expected if polymerisation of the film was temperature dependent.

Figure 35 has collected the film thickness values for the experiments reported earlier where the temperature was taken from  $20 - 250^\circ\text{C}$  in steps of  $25^\circ\text{C}$ . There is a very noticeable change in the trend at around  $180^\circ\text{C}$ , where the film thickness drops appreciably. In some cases, above  $200^\circ\text{C}$ , the film became disrupted and readings were no longer obtainable. In one experiment, the film failed at  $250^\circ\text{C}$  and resulted in a scuff - the friction rose sharply and the noise increased as well. This is shown in Figure 36 for oil A at 1 kg. In this particular case, the film disruption started at about  $175^\circ\text{C}$ , and the friction trace was seen to fluctuate as the film began to break down.

In the cylinder-liner experiments, there is a visually noticeable difference between the surfaces run at 50°C, and the surfaces run at 150°C (see Figure 23). This indicates that the ZDDPs have provided a better protection at this temperature. On going to 200°C in separate experiments, there does seem to be a slight reduction in the effectiveness of the additive. This certainly ties up with the observations of electrical contact resistance and friction in these experiments. Figures 37 and 38 show the superimposed e.c.r., friction and temperature traces for the experiments that produced the photographs in Figure 23. Very clearly, the average electrical contact resistance is highest (indicating a thicker and more coherent film) at 150°C. At either 50°C or 200°C, the film quality is noticeably worse. This is most clearly shown with oil B (Figure 37), where there is almost zero e.c.r. at 50°C, and greatly disrupted at 200°C.

#### 5.5 Shear Properties of the Reaction Films

The results presented indicate that the reaction films formed with ZDDP in these experiments did not behave in a viscous manner. The behaviour in the contact is more consistent with a solid polymerised film. Under sliding conditions, the film behaves plastically - as a solid with a constant shear strength. This being the case, deductions about the shear strength should be available from friction force data.

It is assumed that the reaction films have reduced the frequency of metallic contact to such an extent that the contribution of such asperity interaction to the total friction force is negligible. Our results of capacitance measurements show this to be a good assumption. This then means that the friction force measured is due to the shearing of the film itself. The second interim report [18] included a simple calculation of the shear strength of such a film by dividing the friction force in

an experiment by the area of the wear scar - determined by a measurement of the wear scar diameter on the ball. Repeating and extending this calculation for the range of additives gives values of shear strength in the range 50 MN/m<sup>2</sup> to 100 MN/m<sup>2</sup> (Table 4). The shear strengths of the films seem to be roughly comparable.

Workers in the field of thin polymeric films on a hard substrate [29, 30] have suggested a relationship between the measured contact shear force and a shear strength of the film. It has the form:

$$\tau_c = \tau_0 + \alpha p$$

where  $\tau_c$  is the shear strength measured,  $\tau_0$  is a constant shear strength for the material,  $\alpha$  is a constant and  $p$  is the contact pressure. It is not clear that our reaction films behave in this way: there is no definite evidence for a  $\tau_0$ , but there is some indication in our experiments that the reaction films behave in this way, but experimental accuracy at the moment is not enough to decide. Modifications to the sensitivity of friction-force measurement to take this idea further is now being undertaken.

## 6 DISCUSSION

The apparatus described here has enabled the reaction film thickness of ZDDP additives incorporated in a base oil to be measured under the four conditions considered necessary in the introduction, namely;

- (i) The film formed in a rubbing contact
- (ii) Realistic surfaces and materials used
- (iii) The temperature of the contact known accurately
- (iv) Lubrication conditions known, to be boundary with minimal hydrodynamic component.

These experiments have shown that both temperature and rubbing are necessary for the formation of the reaction films from ZDDP. The second interim report [18] described how no evidence of any reaction film being formed away from the wear scar was found. This was demonstrated there by using x-ray diffraction analysis and looking for the elements in the additive that were expected to appear in the film (namely Zn, P and S). The film formed only where there was rubbing. Recent infra-red studies of rubbed reaction films confirm this observation [25]. Here the important role of temperature in sustaining the reaction of the additive and promoting film formation has been shown. Since the contact temperature is known accurately, conditions under which the film forms have been observed. It appears that the additives can become active at moderately low temperatures (75°C) but that they form the best films in the region of 150 - 200°C. This reflects the thermal stability of the additives. Above 200°C they decompose, and this hinders the formation of the film.

The implication in practice, and particularly in the piston ring/cylinder liner contact, is that the ZDDPs act over a large range of temperature. It is thought that typical liner wall temperatures range from 150 - 250°C (although accurate measurement is absent). At the top of this range,

the ZDDP film is becoming disorientated, and thermal decomposition hinders the anti-wear activity. It should be noted, of course, that the ZDDP additive is never used on its own, and the inclusion of other additives tends to mask the individual contribution [26, 27].

#### 6.1 Film Formation and Wear Reduction

At the onset of rubbing, there was no reaction film in the contact. The observed initial 'induction' time when no film activity was detectable has been reported elsewhere [5], and is probably due to the initial run-in conditions being too severe to sustain a film. However, the subsequent rapid film formation leading to a protective film indicates that these extreme conditions do not last long. It is in the first few minutes that the degree of solid-solid contact is highest, and when most of the wear takes place. This was noted when commenting on the variable time experiments with cast-iron cylinder liners (Figure 24) in the results section. The wear scars are very similar after 5 minutes and after 2 hours. This observation has important implications for the running-in procedures in diesel engines.

Clearly not all the wear takes place in the first 5 minutes, and in the cast-iron experiments it is very evident that asperity interaction continues even for 2 hours of running. This was detected from observations of the capacitance signal being shorted-out at many points. As the experiments proceed, the running-in process continues, and presumably there are significant changes in the surface topography. These observations are the impetus for the next stage of the work, looking at the topographical changes during running in, and the scheme is outlined in the Appendix.

In experiments on the polished-steel specimens as well as on the cast-iron specimens, the reaction film was found to be highly tolerant of changes in operating conditions. This is particularly noticeable in

the variable load experiments. A new load-stage often produced a disruption in the film - evidenced by a sharp drop in the electrical contact resistance, corresponding to a sudden increase in asperities interaction. However, the electrical contact resistance was observed subsequently to rise rapidly to its high value again indicating rapid film re-formation, and the maintenance of anti-wear protection. This is also important in running engines, since conditions in the piston ring contact are seldom steady. The reaction film quickly responds to changes in the contact conditions.

It has long been held that the major importance of an additive such as ZDDP is in wear reduction, and only secondarily in friction reduction. All these experiments have demonstrated this to be the case. The friction coefficient is a bad indicator for the performance of the additive. Here, the base oil alone had a friction coefficient of the same size as base oil + additive, a value around 0.1 in all experiments. The friction coefficient remained at this value, even when all metallic contact had ceased.

## 6.2 Film Properties

We have observed that the main function of the ZDDP is that of wear reduction. Shearing of the metal surfaces or asperities in the contact is replaced by shearing of this solid reaction film. Although static loading tests on the film formed in the contact shows some elastic behaviour (the film thickness is the same on loading as when unloading), it cannot be the elastic properties that contribute to wear reduction. The film is in gross shearing for most of the contact time, it is only 'static' at the ends of the stroke. It must therefore be the plastic behaviour of the films that is important in the contact, and the way the film is bonded to the surfaces that determines its effectiveness as a wear-reducer. The infra-red studies mentioned earlier [25] indicate that the additive

is strongly bonded to the metal substrate, but that there is a less-strongly held part of the film that is possibly a polymerised layer.

The reaction films formed in these tests were found to be solids, remaining in the contact when motion was removed. They behaved elastically under normal load, and as constant shear strength material under tangential motion. Their plastic behaviour seems to be similar to that of some common extruded polymers such as PMMA and HDPE. The shear strain rates in these experiments are high (of the order  $10^6 \text{ s}^{-1}$ ) and are comparable to the extrusion process. Further experimentation is needed to investigate the shear properties of these films.

It was noted that when the film was loaded dynamically, the film thickness reduced, and also that the film thickness was greater at the ends of the motion (where the velocity is zero) than at mid-stroke. This has been attributed to a "bull-dozing" action of the slider, shearing and pushing the films to the ends of the contact. The slider then rides-up on these heaps of material.

Film thicknesses in these experiments have been deduced to be in the range  $0.05 \mu\text{m} - 1.0 \mu\text{m}$ . These values of thickness are of the same order as films formed by elastohydrodynamic lubrication of concentrated contacts. However, these results have demonstrated that the apparatus functions in the boundary lubrication regime, i.e. that there are no viscous effects. As boundary films, the reaction films are thick, much greater than a 'traditional' boundary film of a few molecular layers. The evidence is that there is a polymerised solid in the contact. The film thickness is generally larger than the surface roughness of the wear scars. At higher loads, the deduced thickness becomes comparable with the roughness. The film remained effective in wear reduction. This remained the case when no film thickness values were obtained (i.e. that film thickness was less than roughness size) with cast-iron liner specimens.

### 6.3 Effect of Temperature

For the constant temperature of 150°C, it has been observed that there is a variation in the thickness of the reaction film between different ZDDPs used. The four additives can be ranked roughly in the order C, (B/D), A of decreasing film thickness at constant load. Looking at the composition of the additives we see that this trend is reflected in the thermal stability and reactivity of the additives.

Oil C contains a secondary alkyl ZDDP which, when compared with oil A which contains a primary alkyl ZDDP (see Table 1), had a higher reactivity and a lower thermal stability. From this viewpoint, oil C would be expected to react at a lower temperature and to produce thicker films than oil A. This is found to be the case. The placing of oils B and D in the ranking are not clear from the experiments, and as yet details of their relative reactivity and thermal stability are not available. The observation that the nature of the alkyl group affects the thickness of the reaction film formed has recently been indirectly observed using surface analysis techniques [28]. The authors there indicate that while the surface composition for different additives is the same (also indicating a polymerised upper layer on a more tightly held lower layer), the thicknesses are different for different alkyl groups in the ZDDP. Their results tend to the same qualitative picture as deduced here.

The difference in film thickness on going from conditions at 100°C to conditions at 200°C has seemed fairly minimal. If anything, there is a slight increase in the film thickness at 200°C over the value at 150°C or 100°C. This again reflects the reactivity and thermal stability of the additive. Particularly in the polished steel specimens a marked decrease in film thickness was observed at 180 - 200°C, which corresponds to the temperature at which the additive begins to decompose. Together with this film thickness decrease, increased asperity action produces a small increase in wear.

## 7 CONCLUSIONS

The apparatus described in this report has enabled thickness measurements of reaction films formed by ZDDP during the running process to be made, using capacitance.

The apparatus functions under the four conditions considered necessary in the introduction. Working with these conditions of rubbing contact, realistic surfaces, known contact temperature and known lubrication regime some new features of the formation and thickness of reaction films have been found.

Reaction film thicknesses were deduced to be in the range  $0.05 \mu\text{m}$  -  $1.0 \mu\text{m}$ . These were comparable or greater than the apparent surface roughness of the wear scars.

These film thicknesses are typical of values in the ehl regime. Films of this size are not formed by hydrodynamic action, but by polymerisation of the additive on active metal surface produced by rubbing.

Reaction film formation is rapid, taking place in the first few minutes of sliding. The film is continuous across the stroke once formed, and remains in the contact when motion is stopped. Film thickness is almost constant across the stroke, being greater at the ends of the stroke due to a piling-up effect.

The reaction films formed in these experiments were found to be solids. They behaved elastically under normal load, and as constant shear-strength material; under tangential motion. The shear strengths are similar to common extruded polymers such as PMMA and HDPE.

Reaction film thickness and film quality vary according to the temperature of the contact. The films protect the surfaces best in the range  $150 - 200^\circ\text{C}$ . The film thickness is affected by the nature of the alkyl group on the ZDDP. Those with a lower thermal stability and higher

reactivity produce the thicker films.

Once formed, the films show a remarkable tenacity and can rapidly respond to fluctuations in load, and hence in contact conditions.

These observations have important implications for the lubrication of engine parts such as cylinder liner/piston ring and in running-in procedures in engines. They also contribute to our understanding of the role of reaction films in boundary lubrication.

The next stage of the research will concentrate on the running-in process using cast-iron cylinder liners. The aim will be to gain a better understanding of what makes a 'good' run-in surface, and particular attention will be made to changes in surface topography. The primary aim is to relate the performance of these test liners to that of the same liners and additives in full-scale tests (see Appendix).


ZDDP		ANALYSIS
OIL A	PRIMARY $-(\text{CH}_2)_{34}\text{CH}_3$	PARANOX 15 Zinc 9 Sulphur 11
OIL B	PRIMARY $-(\text{CH}_2)_{11}\text{CH}_3$	PARANOX 16 Zinc 7.7 Sulphur 9.8 Phosphorus 7.7
OIL C	SECONDARY $(\text{CH}_3)_2\overset{1}{\text{C}}\text{HCH}_2\text{CH}_3$	LUBRIZOL 677A Zinc 8.85 Sulphur 17 Phosphorus 8.3
OIL D	ALKYL ARYL $-(\text{CH}_2)_{11}\text{CH}_2$ 	LUBRIZOL 1376A Zinc 8.5 Sulphur 12.3 Phosphorus 6.4

TABLE 1

DETAILS OF THE ADDITIVES

R 4.5 mm PIN AT 150°C		
	$\mu$	$\phi$ mm
BASE OIL	0.133	0.497
	0.125	0.610
OIL A	0.122	0.159
	0.135	0.205
OIL B	0.097	0.116
	0.104	0.137
OIL C	0.109	0.155
	0.108	0.157
OIL D	0.103	0.145
	0.105	0.109

TABLE 2

COMPARISON OF WEAR SCAR DIMETERS ( $\phi$ ) AND FRICTION COEFFICIENTS FOR THE BASE OIL ALONE AND WITH ADDITIVES

1.0 Kg		NO ADDITIVE	ADDITIVE A	ADDITIVE B	ADDITIVE C	ADDITIVE D
WORN PROFILES						
FILM THICKNESS $\mu\text{m}$		NO FILM	0.34	0.34	0.55	0.19
WEAR SCAR DIAMETER mm		0.197	0.126	0.107	0.111	0.150
0.2 Kg						
WORN PROFILES						
FILM THICKNESS $\mu\text{m}$		NO FILM	0.54	0.66	0.62	0.68
WEAR SCAR DIAMETER mm		0.135	0.083	0.084	0.067	0.073

TABLE 3  
WEAR PROFILES AND FILM THICKNESSES

R 4.5 mm PIN AT 150°C	
	Shear strength of contact (MPa)
OIL A	41 80
OIL B	54 58
OIL C	58 125
OIL D	45 113

TABLE 4

SHEAR STRENGTHS OF REACTION FILMS

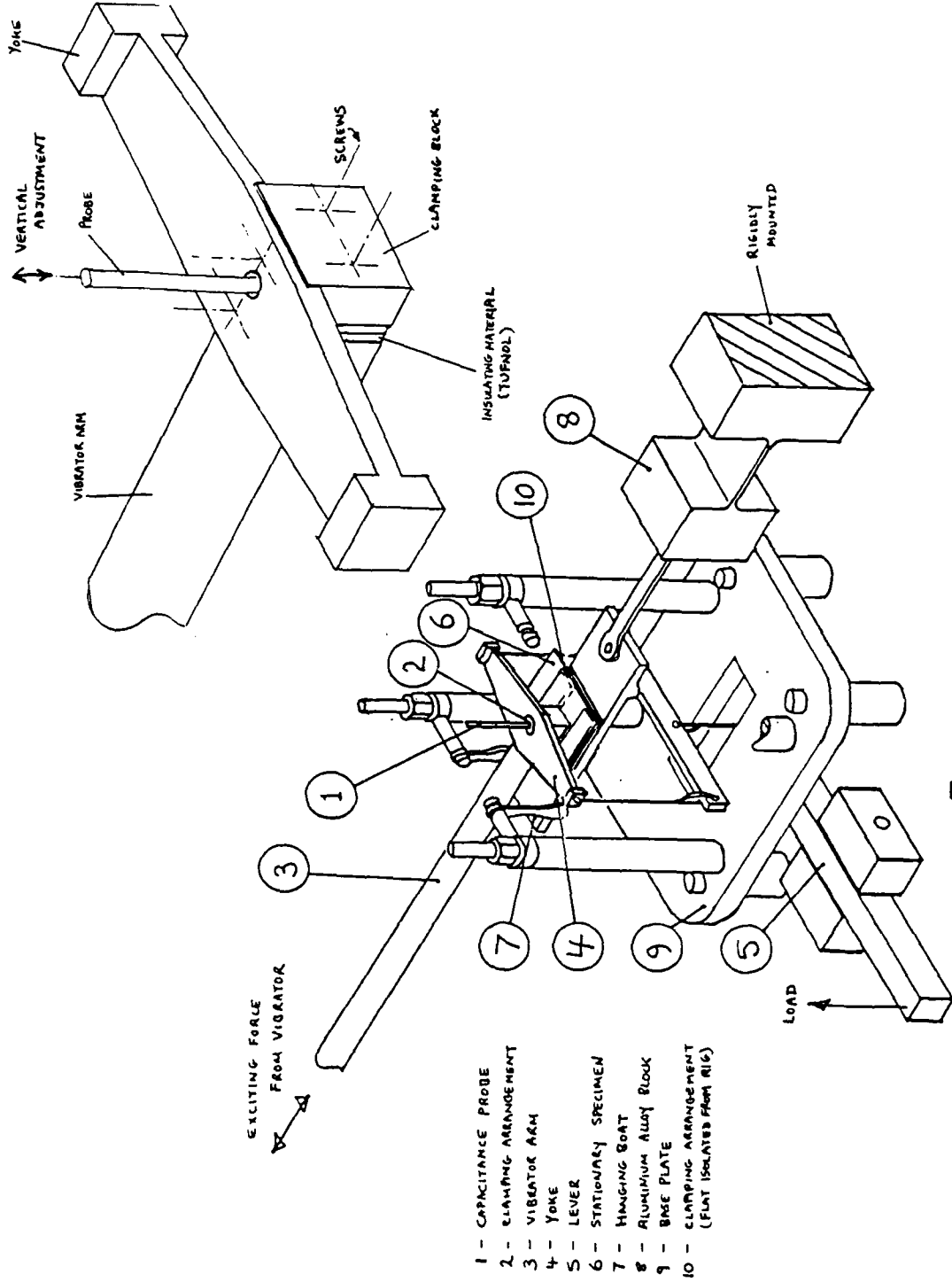


FIGURE 1  
RECIPROCATING CONTACT RIG

- 1 - CAPACITANCE PROBE
- 2 - CLAMPING ARRANGEMENT
- 3 - VIBRATOR ARM
- 4 - YOKE
- 5 - LEVER
- 6 - STATIONARY SPECIMEN
- 7 - HANGING BOAT
- 8 - ALUMINUM ALLOY BLOCK
- 9 - BASE PLATE
- 10 - CLAMPING ARRANGEMENT (FLAT ISOLATED FROM RIG)

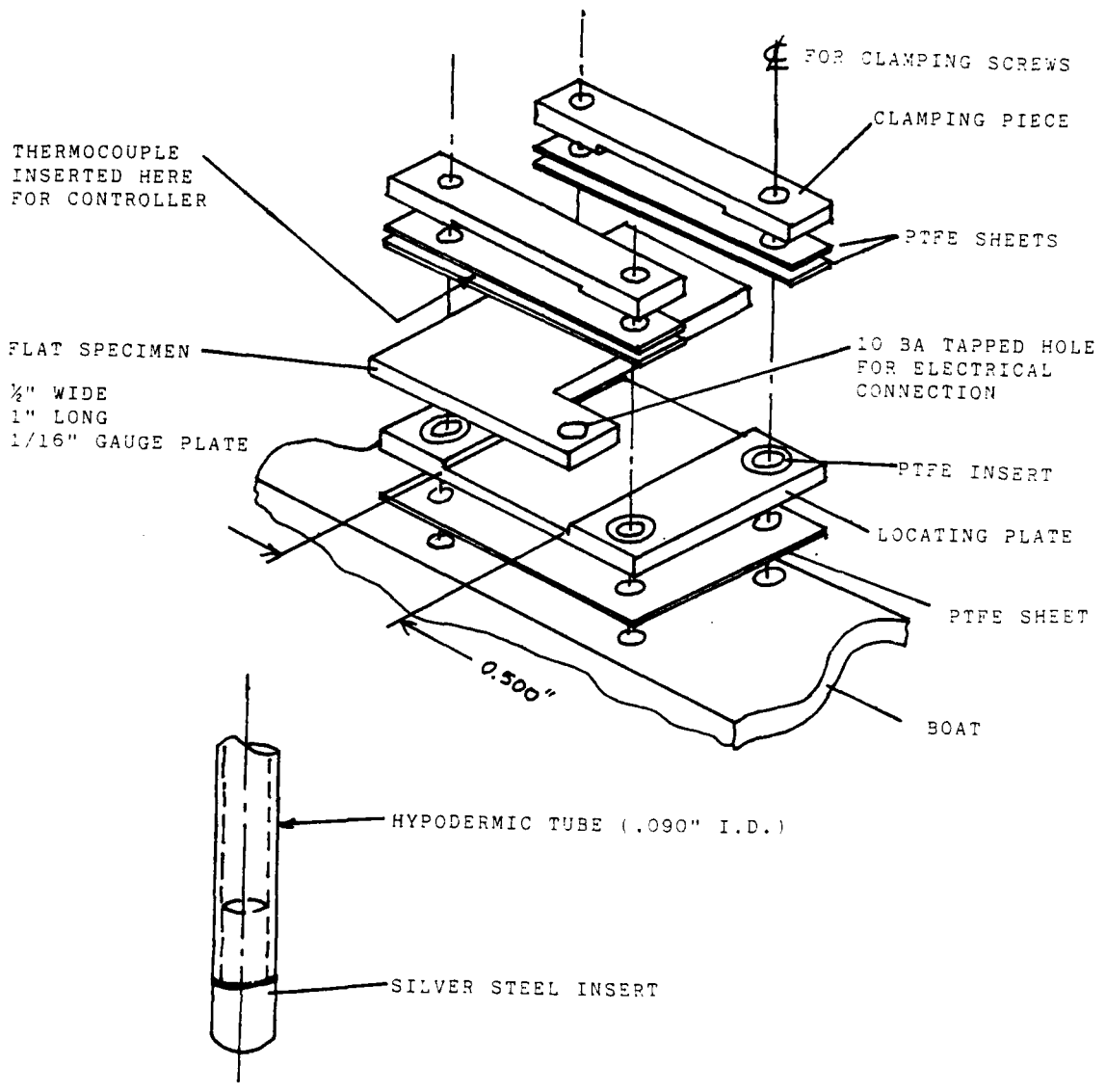


FIGURE 2

DETAILS OF CLAMPING ARRANGEMENT  
 AND PIN SPECIMEN

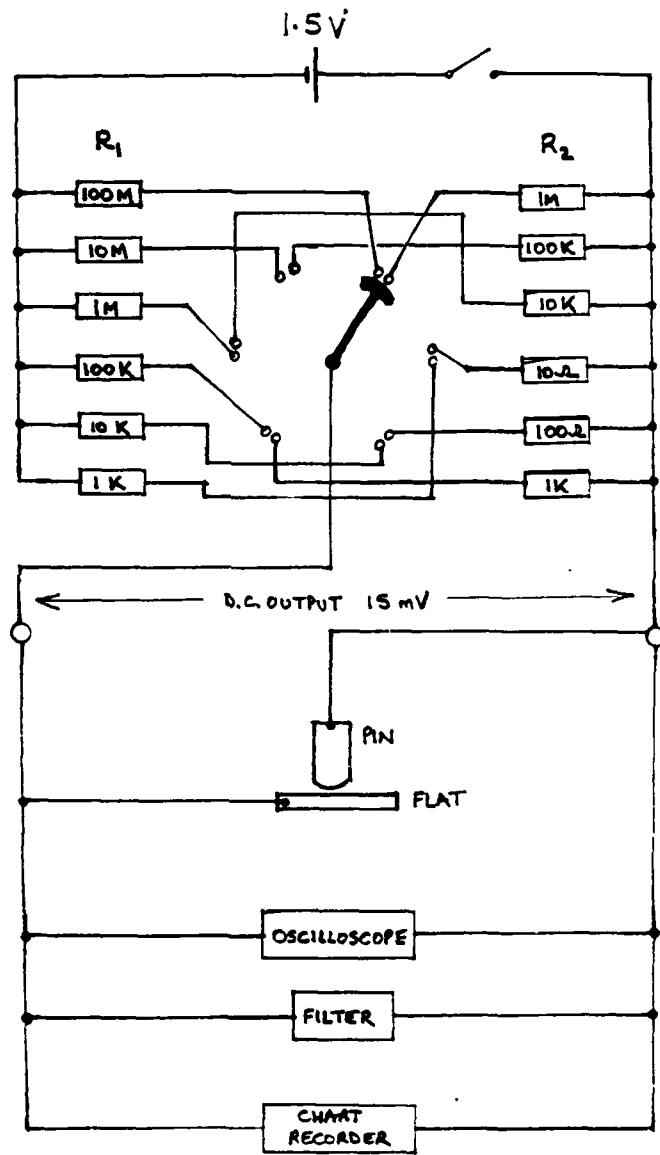


FIGURE 3

PUREY-DUNN TYPE POTENTIOMETER

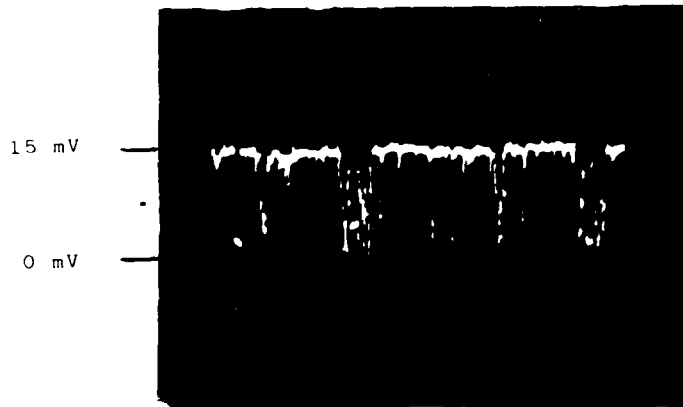


FIGURE 4

TYPICAL CONTACT RESISTANCE PHOTO  
FROM OSCILLOSCOPE

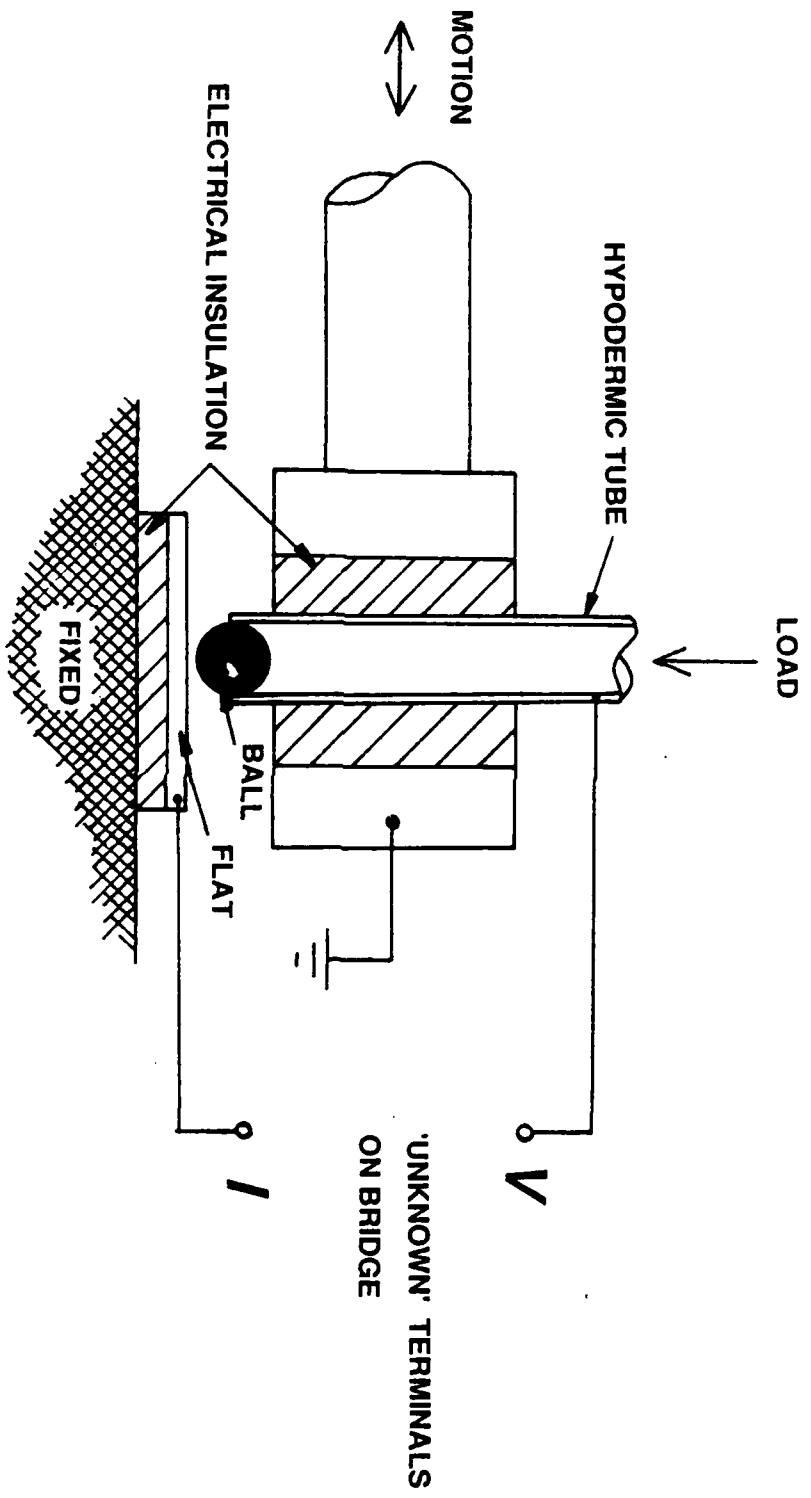
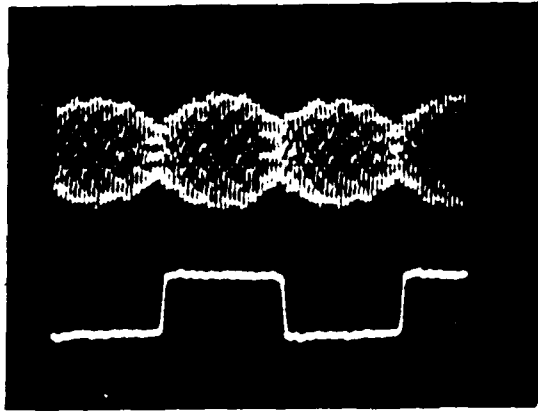
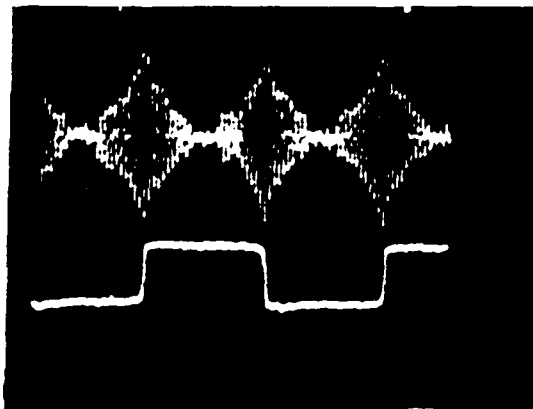


FIGURE 5  
CAPACITANCE MEASURING CIRCUIT



(a)



(b)

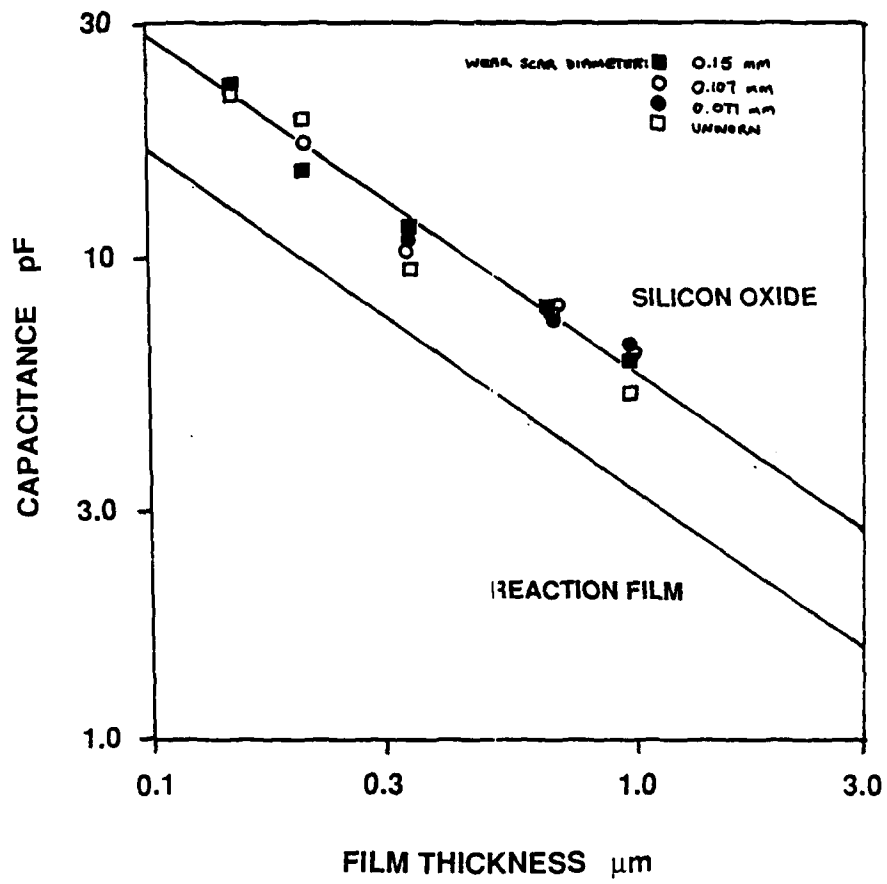


FIGURE 8  
 CALIBRATION CURVE OF CAPACITANCE  
 AGAINST FILM THICKNESS

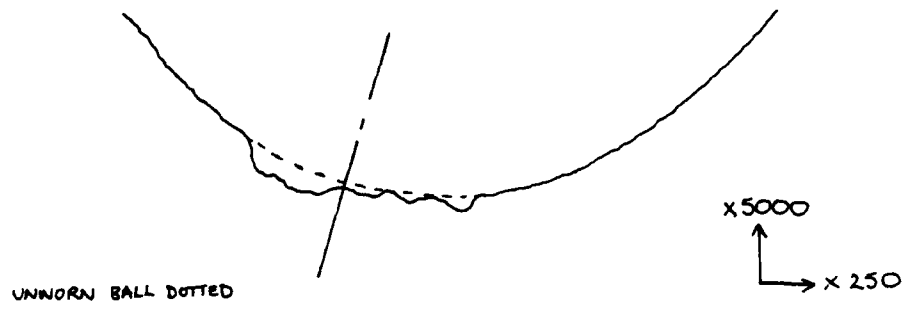


FIGURE 9  
WORN PROFILE OF A BALL

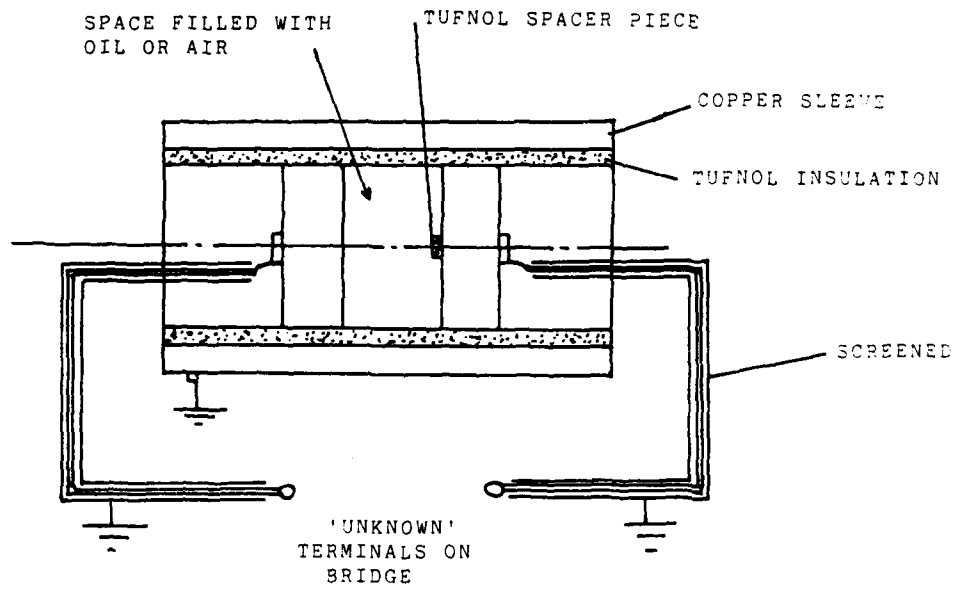
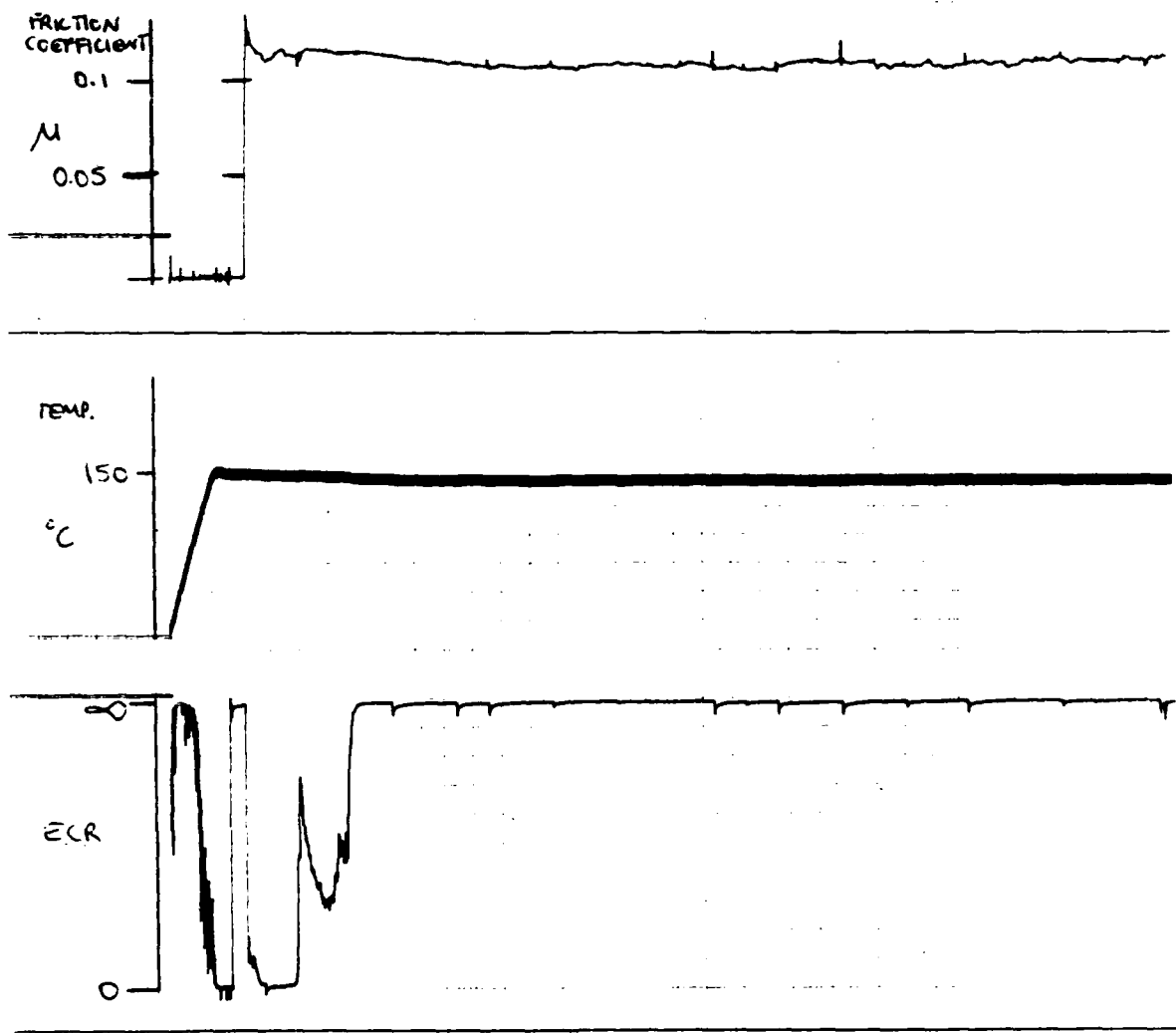


FIGURE 10  
CAPACITANCE CELL



500 SN + 1% LUBRIZOL 677A      RADIUSED PIN ON FLAT  
 ±0.5mm      1 Kg LOAD  
 34.5 HZ

FIGURE 11

FRICITION, TEMPERATURE AND CONTACT RESISTANCE  
 RECORD: CONDITIONS GIVEN

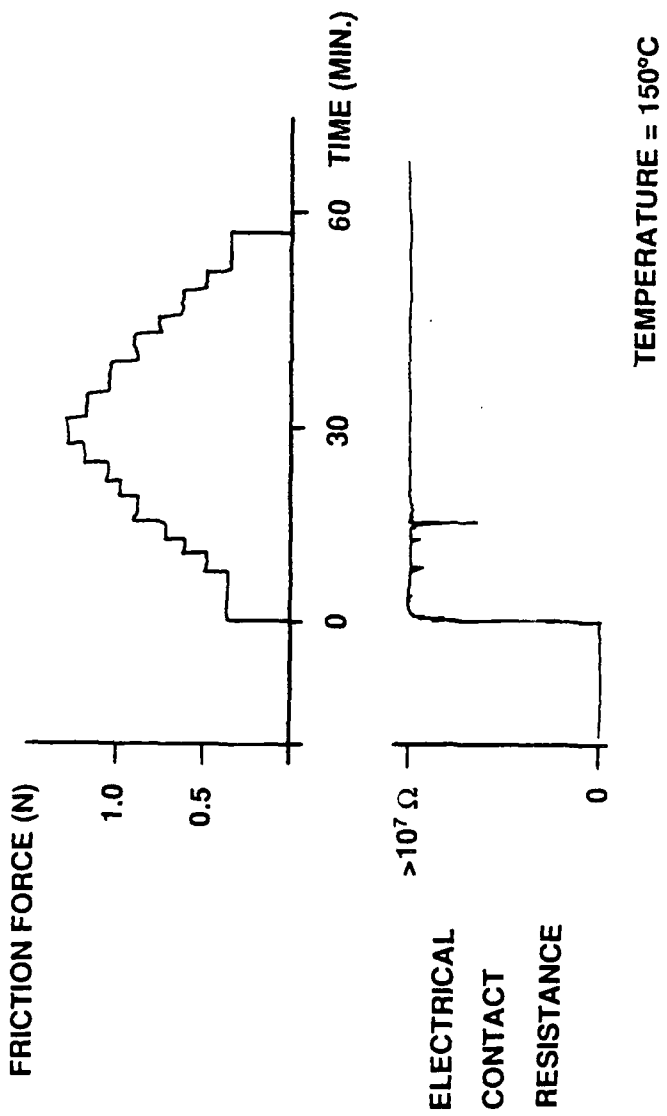
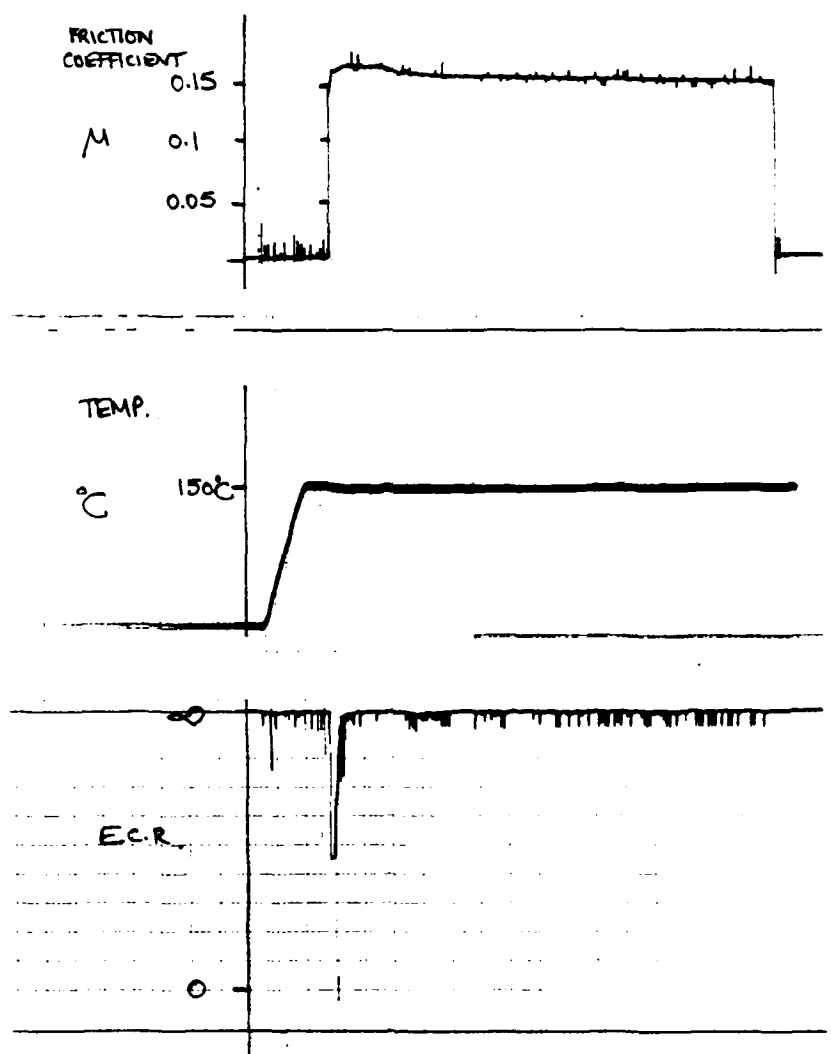
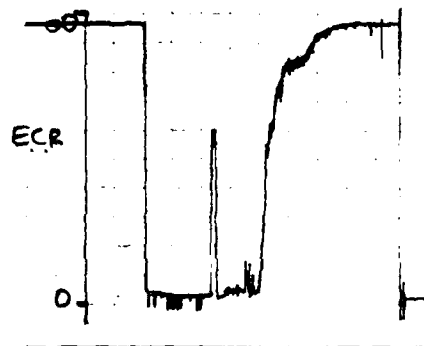
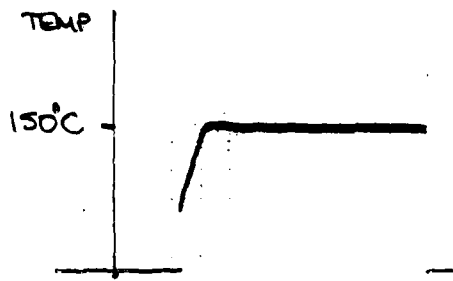
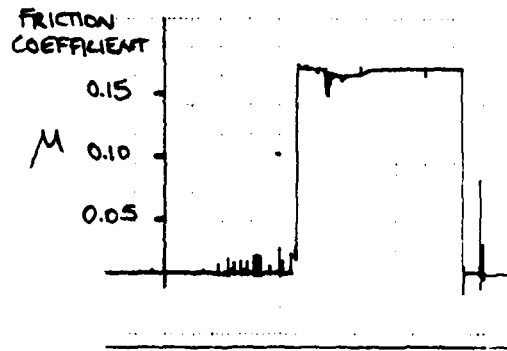


FIGURE 12  
VARIABLE LOAD EXPERIMENT



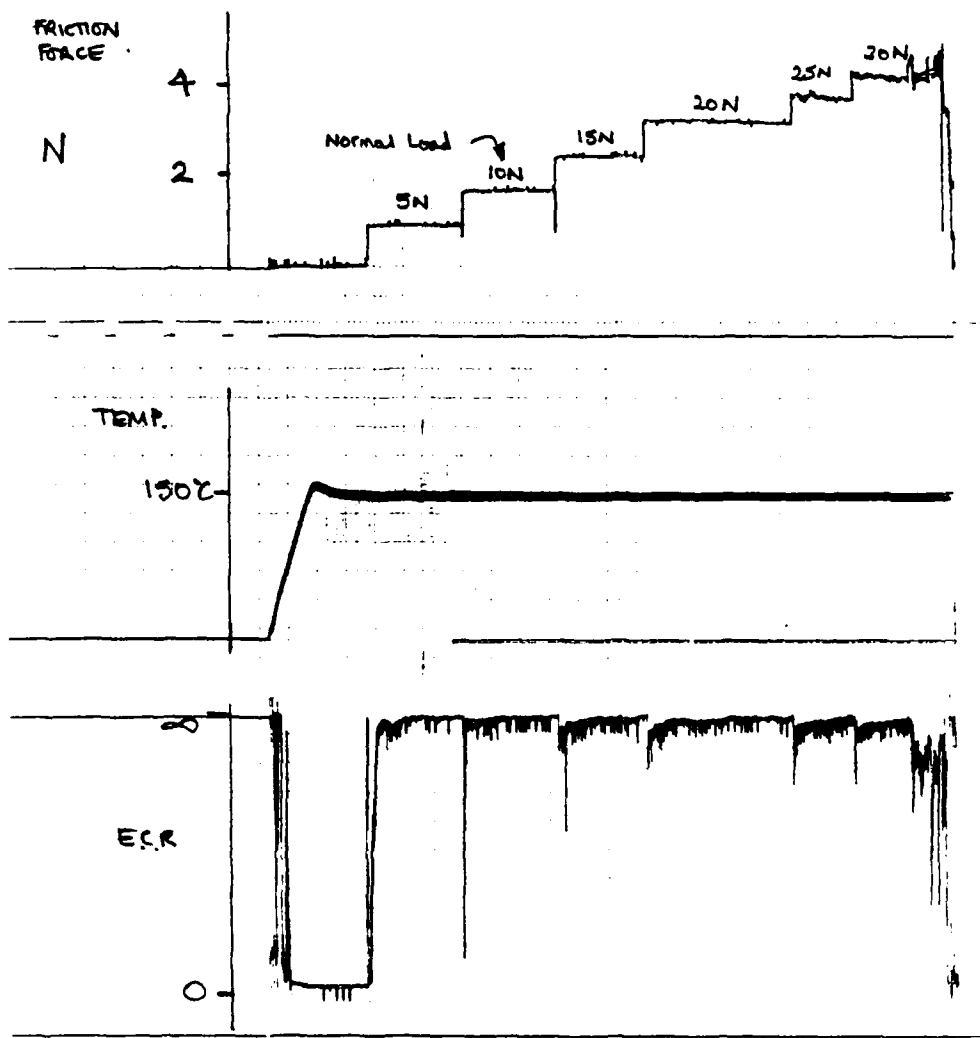
500 SN + 1% PARALDIX 16      RADIUSED PIN ON CAST IRON  
 ±0.5mm  
 34.5 Hz

FIGURE 13



500SN + 17% PRANDX 16      RADUSED PIN ON CAST IRON  
 ± 0.5mm  
 34.5 Hz.

FIGURE 14



500.5N + 1% PARANOX 16      RADIUSED PIN ON CAST IRON  
 ±0.5mm  
 34.5 Hz

FIGURE 15

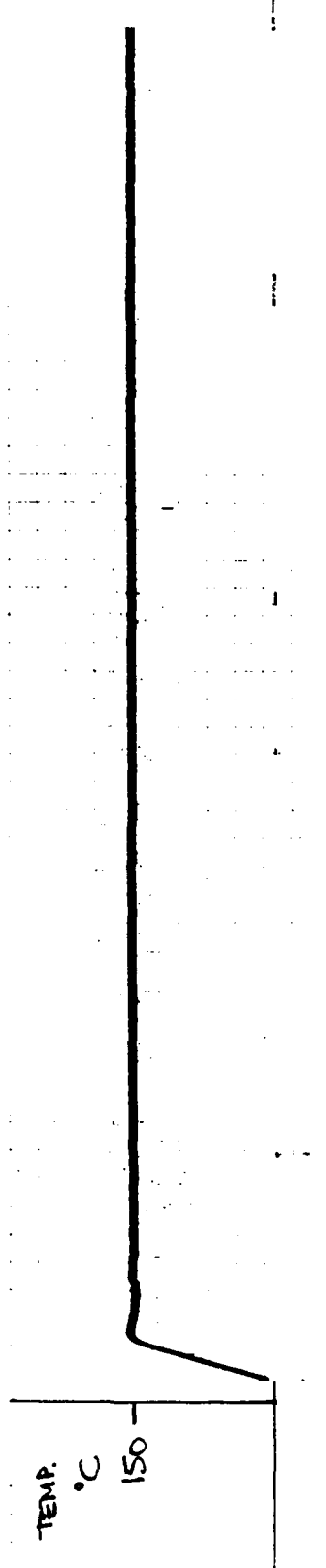
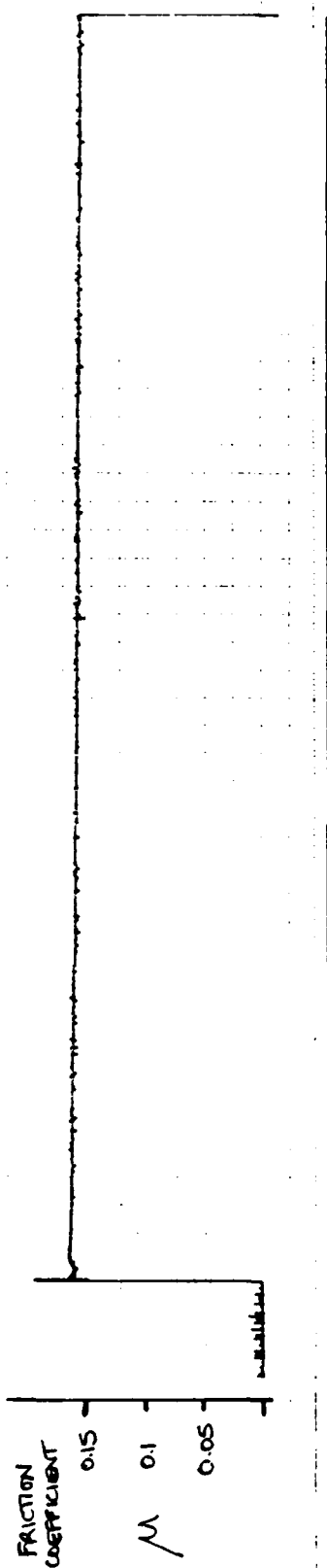
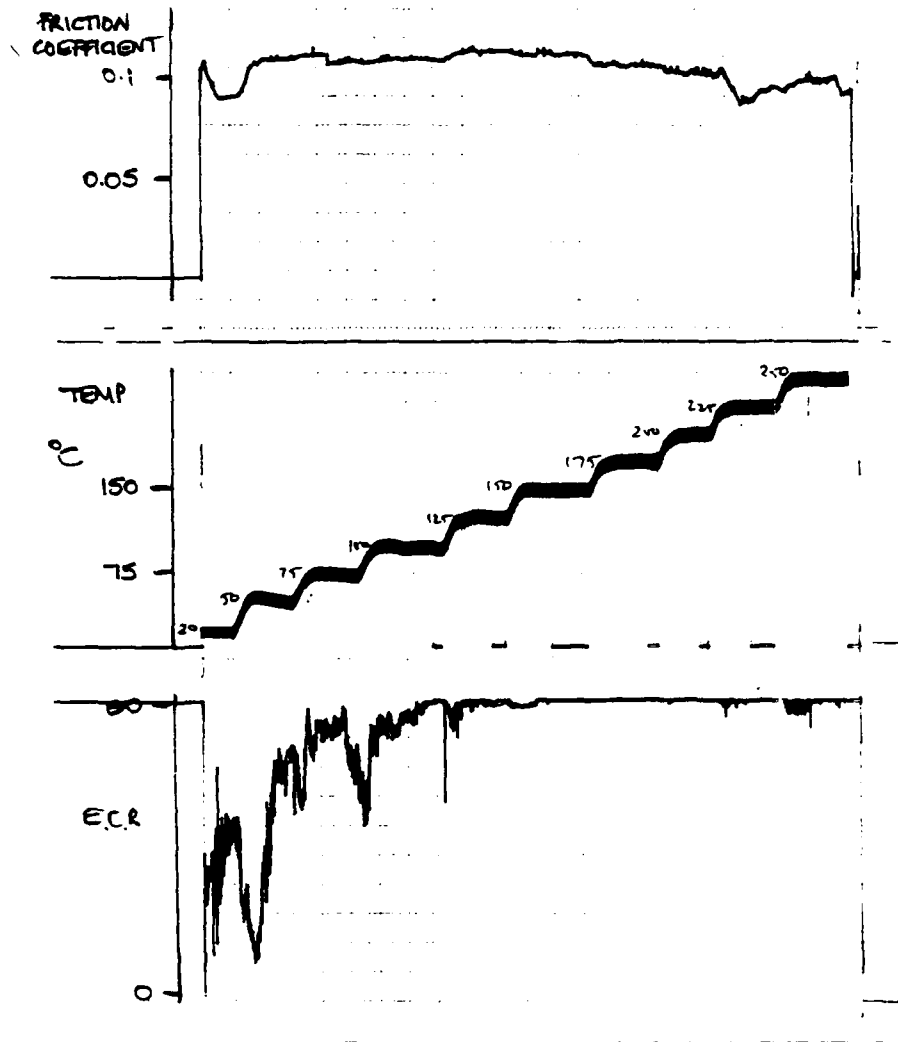


FIGURE 16

500 SN + 1% PHENOLIX 15 REPRODUCED FROM ON CANT IRON  
 ± 0.5 mm  
 34.5 Hz



500SN + 1% PARANOX16      RADIUSED PIN ON STEEL FLAT  
 10.5mm  
 34.5 Hz

FIGURE 10

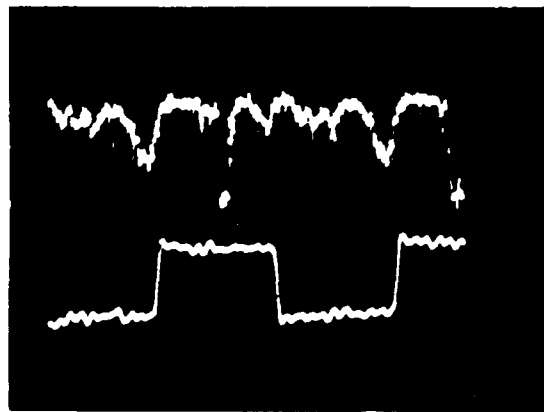
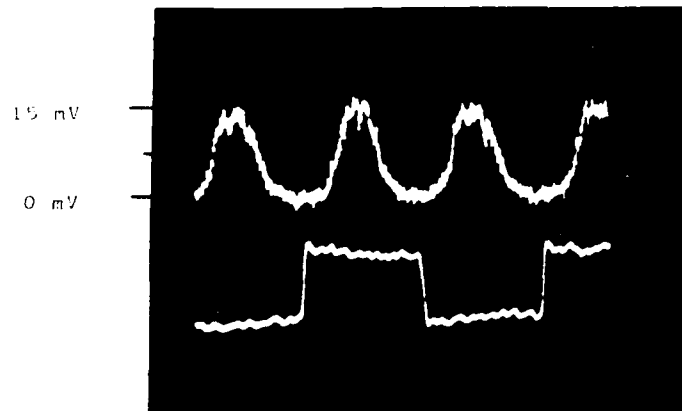
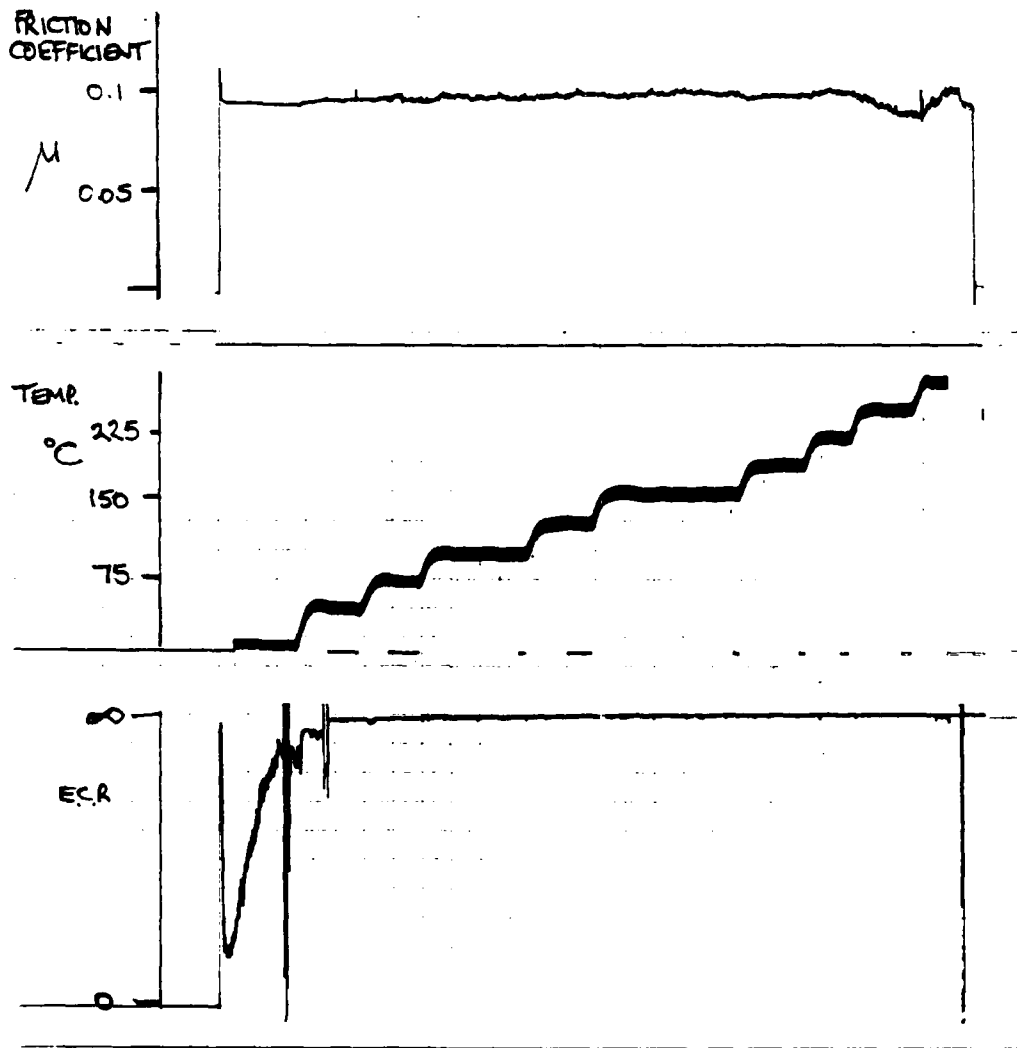


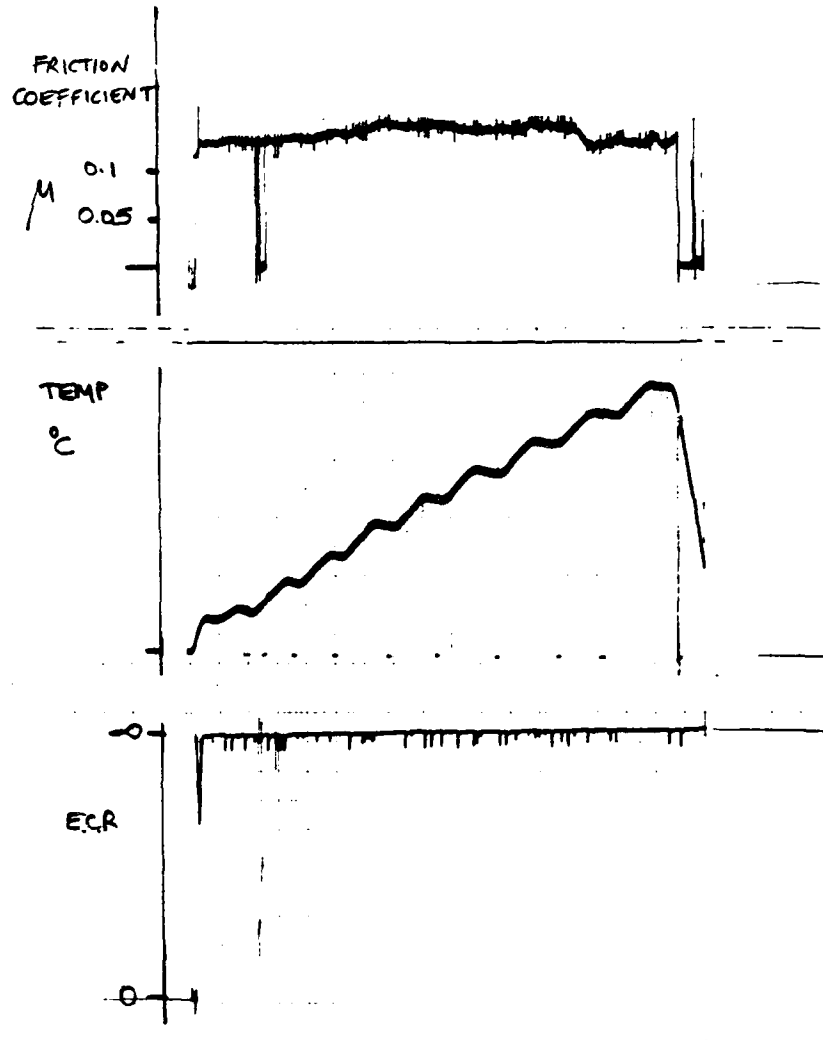
FIGURE 18

FRICITION AND ELECTRICAL SIGNALS  
FROM OSCILLATING MOTOR, SHOWING HYDRODYNAMIC  
ACTION



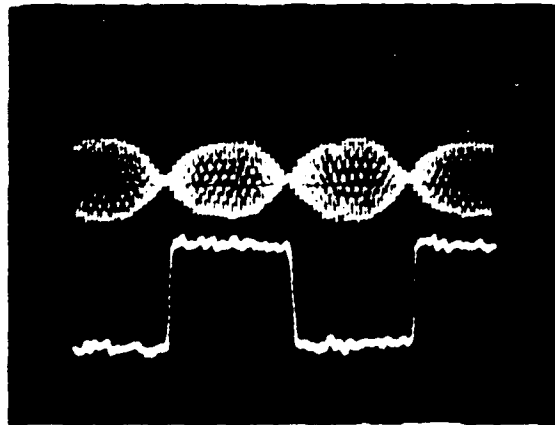
500SN + 1% PARANOX 16 BALL BEARING ON STEEL FLAT  
 10.5mm  
 34.5 Hz.

FIGURE 12



500SN + 1% LUBRIZOL 1376A BALL BEARING ON STEEL FLAT  
 ± 0.5mm  
 34.5 Hz 0.2 kg LOAD

FIGURE 20



RG248E1A1

BRIDGE SIGNAL 'NULLLED' AT ENDS OF PULSES

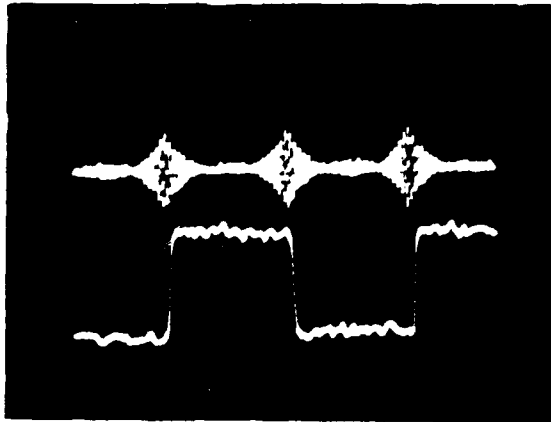


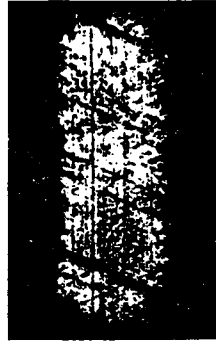
FIGURE 12

BRIDGE SIGNAL 'WIDDED' AT MID-STROKE  
SHOWING FILM SHAPE

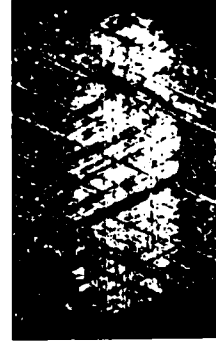
200 °C



RMS ROUGHNESS 4.428  $\mu\text{m}$



RMS ROUGHNESS .476  $\mu\text{m}$



RMS ROUGHNESS .749  $\mu\text{m}$

150 °C



RMS ROUGHNESS 3.114  $\mu\text{m}$

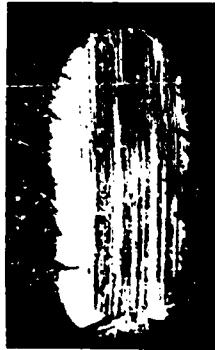


RMS ROUGHNESS .656  $\mu\text{m}$



RMS ROUGHNESS 1.436  $\mu\text{m}$

50 °C



RMS ROUGHNESS 1.886  $\mu\text{m}$



RMS ROUGHNESS 1.057  $\mu\text{m}$



RMS ROUGHNESS 1.506  $\mu\text{m}$

500 SN

500 SN  
+ 1% A

500 SN  
+ 1% B

FIGURE 10

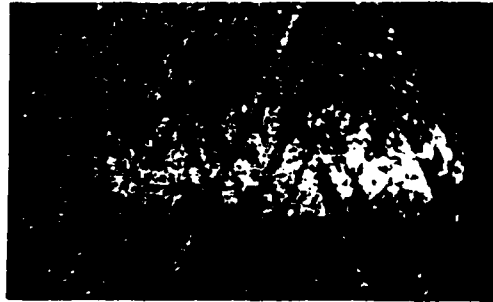
FIGURE 10. PHOTOGRAPHS OF WEAR RECORDS  
AT LOADS OF 100 N, VARIABLE TEMPERATURES

UNKNOWN VALUE  
RMS ROUGHNESS 1.510  $\mu\text{m}$

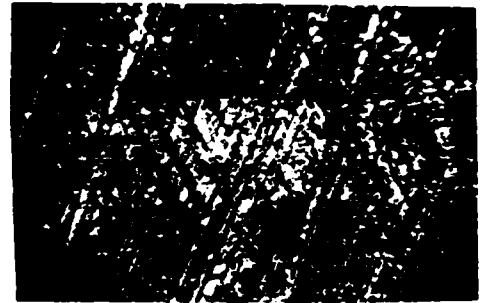
500 SN + 1% PARANOX 15

500 SN + 1% PARANOX 16

5 MINS.



RMS ROUGHNESS 1.181  $\mu\text{m}$



RMS ROUGHNESS 1.344  $\mu\text{m}$

2 HOURS

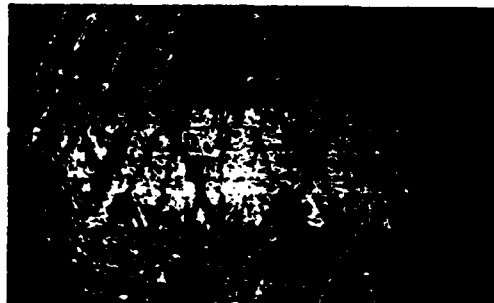


RMS ROUGHNESS .656  $\mu\text{m}$

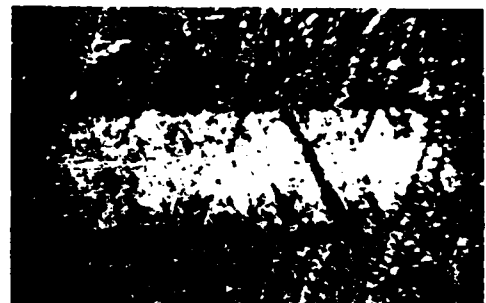


RMS ROUGHNESS 1.436  $\mu\text{m}$

4 HOURS



RMS ROUGHNESS 1.090  $\mu\text{m}$



RMS ROUGHNESS 1.200  $\mu\text{m}$

UNWORN VALUE : RMS ROUGHNESS 1.510  $\mu\text{m}$

FIGURE 24

CAST IRON WEAR RECORD  
VARIABLE RUN-IN TIME

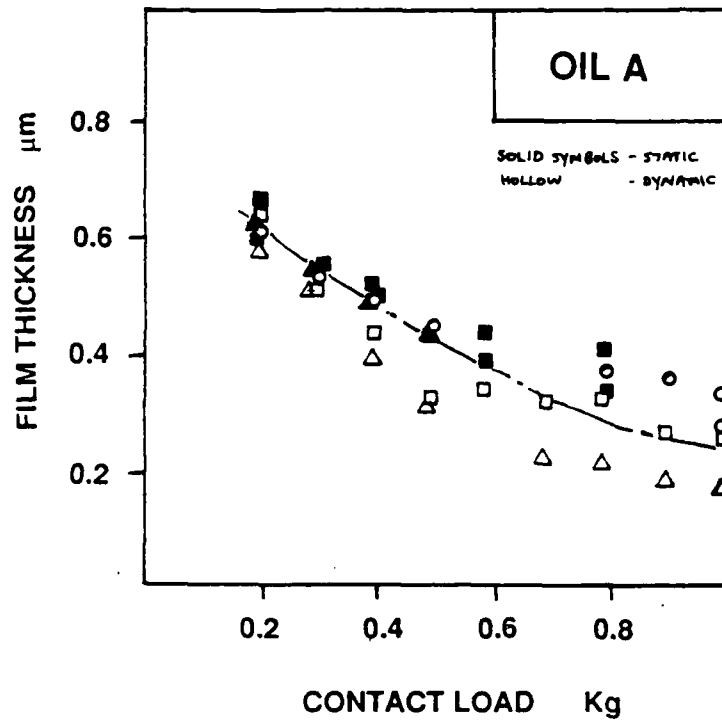


FIGURE 25

OIL A: VARIATION OF STATIC AND DYNAMIC FILM THICKNESS WITH LOAD

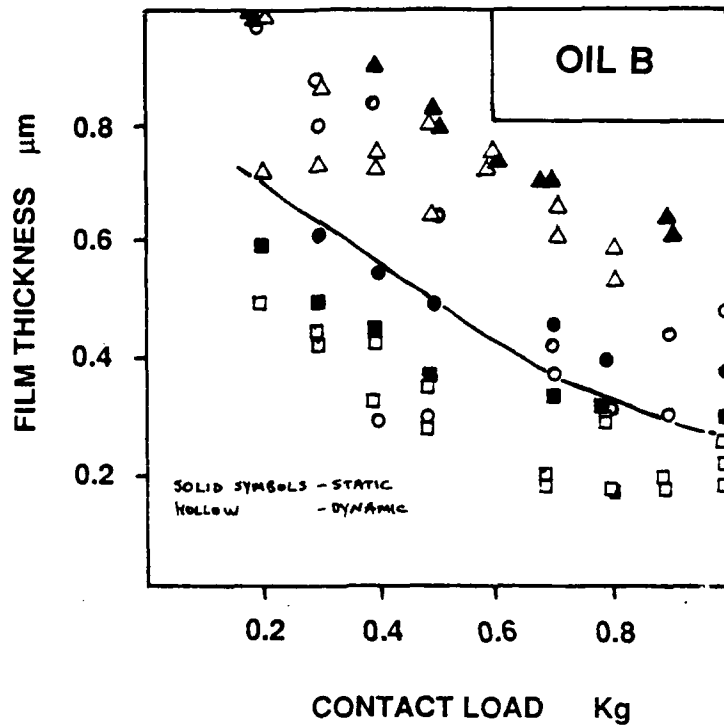


FIGURE 26

OIL B: VARIATION OF STATIC AND DYNAMIC FILM THICKNESS WITH LOAD

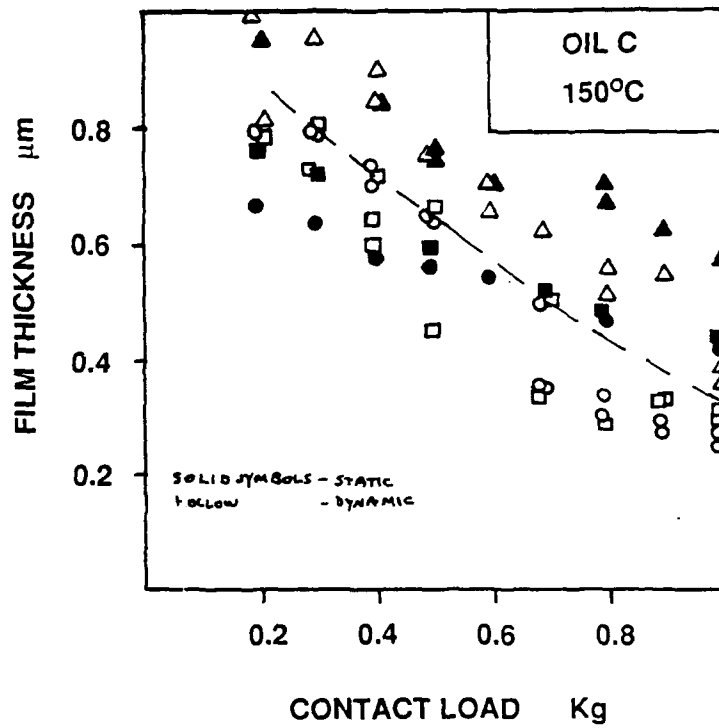


FIGURE 27

OIL C: VARIATION OF STATIC AND DYNAMIC  
FILM THICKNESS WITH LOAD

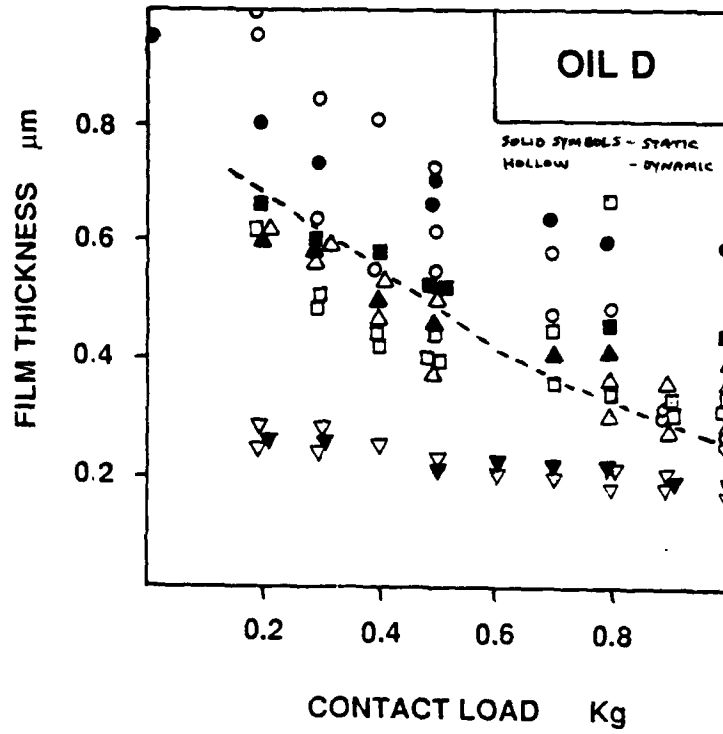


FIGURE 28

OIL D: VARIATION OF STATIC AND DYNAMIC FILM THICKNESS WITH LOAD

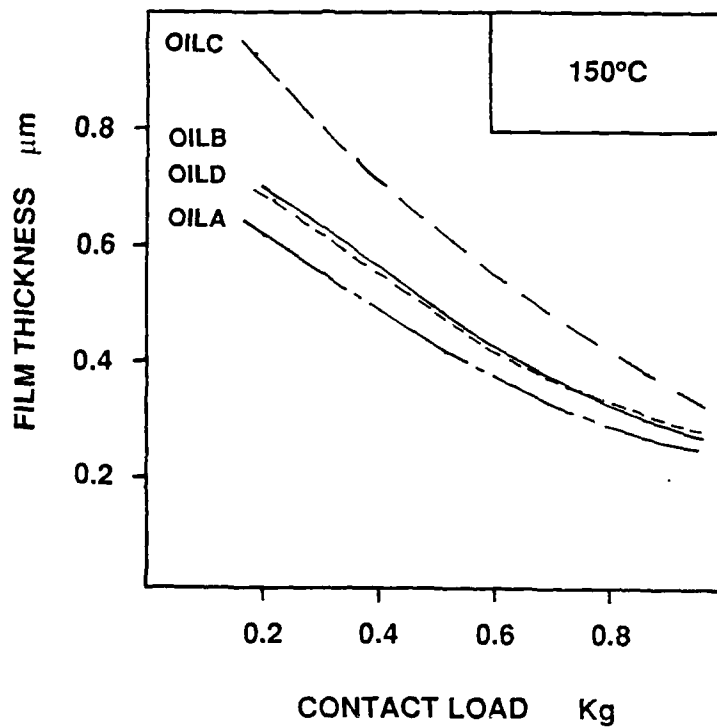


FIGURE 29

COMPARISON OF FILM THICKNESSES BETWEEN  
THE OILS - BALL SPECIMENS

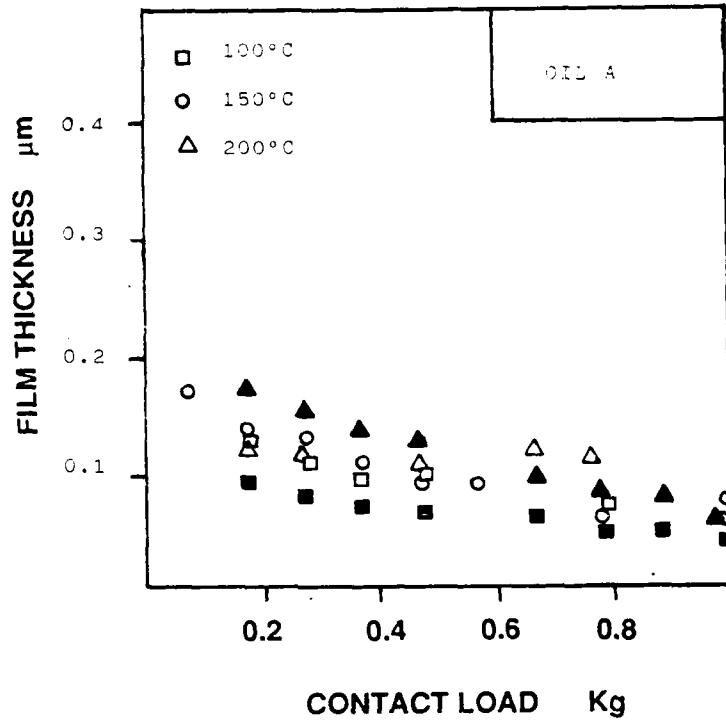


FIGURE 30

OIL A: VARIATION OF FILM THICKNESS WITH LOAD  
RADIUSED SPECIMENS

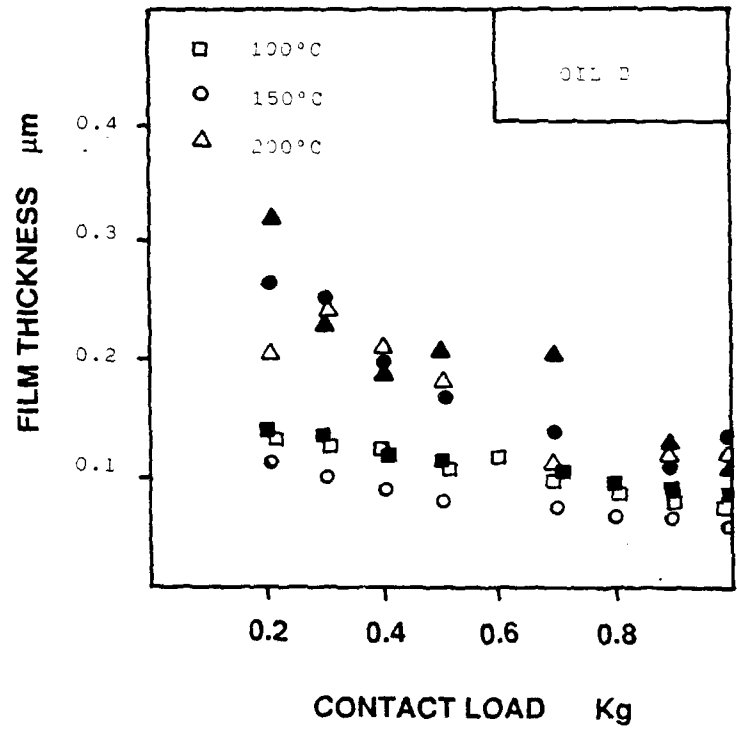


FIGURE 31

OIL B: VARIATION OF FILM THICKNESS WITH LOAD  
RADIUSED SPECIMENS

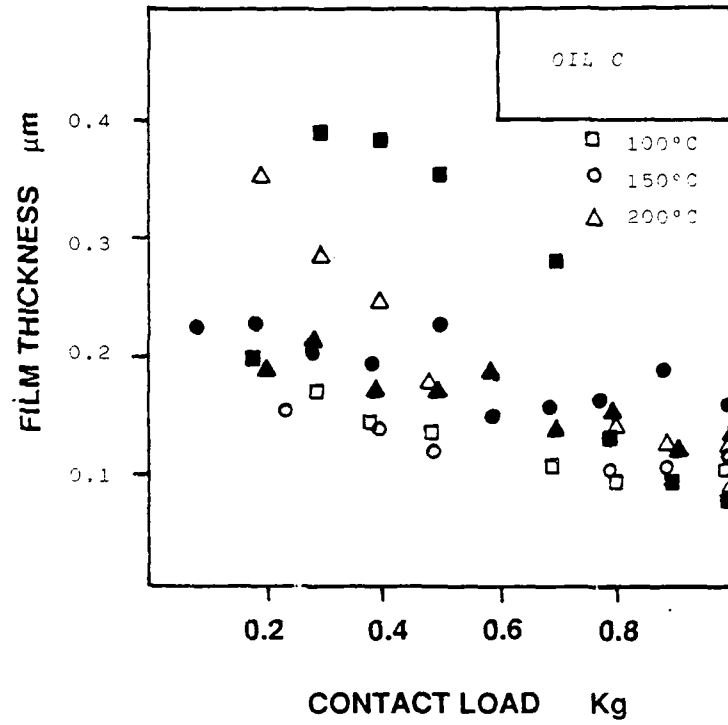


FIGURE 22

OIL C: VARIATION OF FILM THICKNESS WITH LOAD  
RADIUSED SPECIMENS

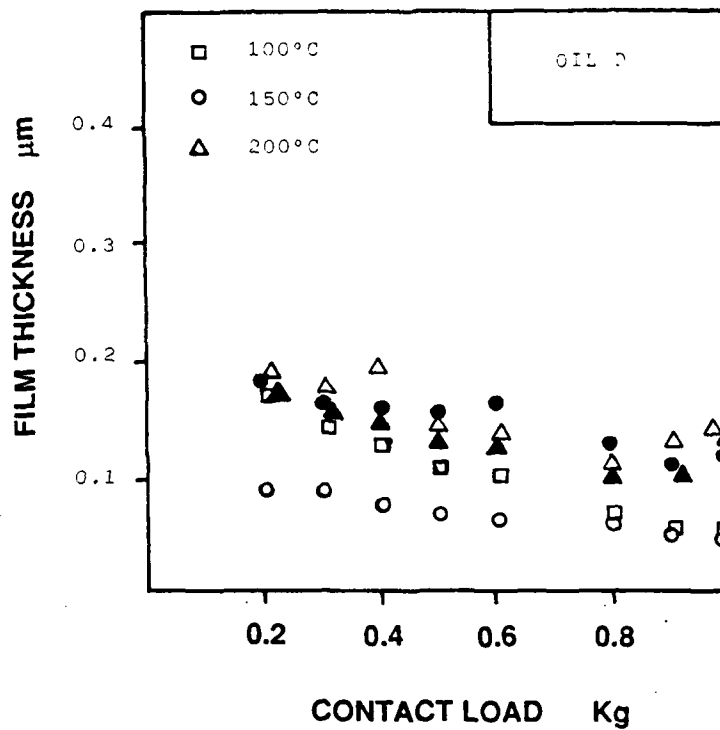


FIGURE 33

OIL D: VARIATION OF FILM THICKNESS WITH LOAD  
RADIUSED SPECIMENS

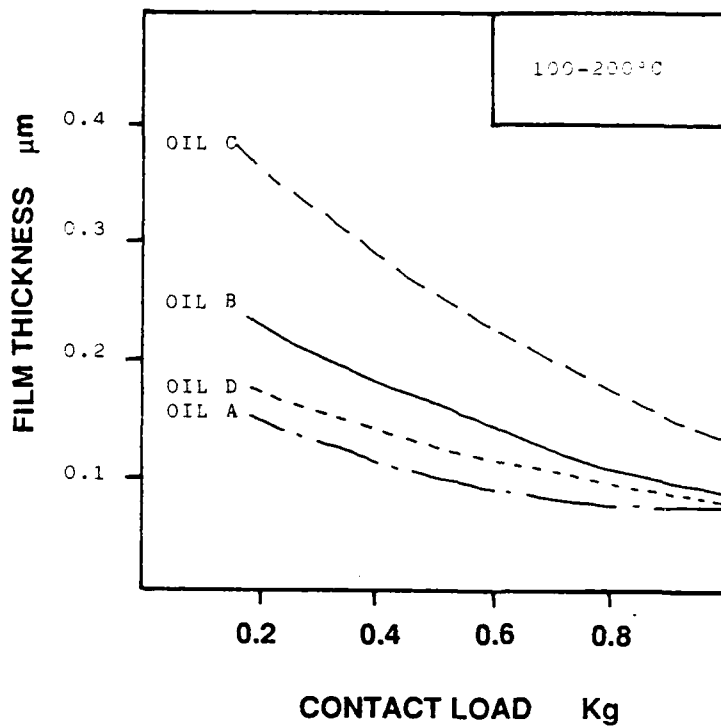


FIGURE 34

COMPARISON OF FILM THICKNESSES BETWEEN THE OILS  
RADIUSED SPECIMENS

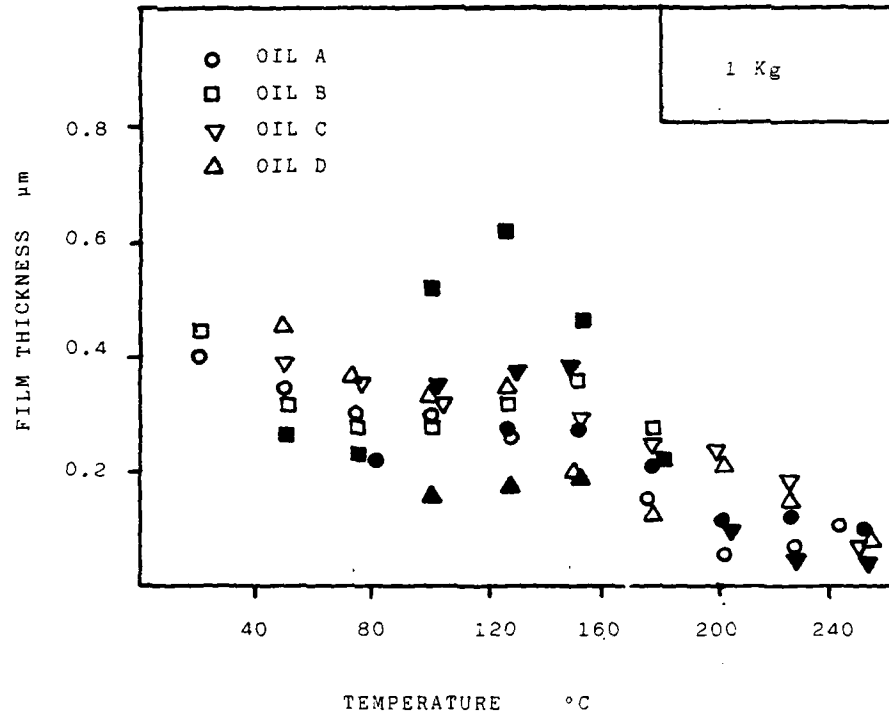
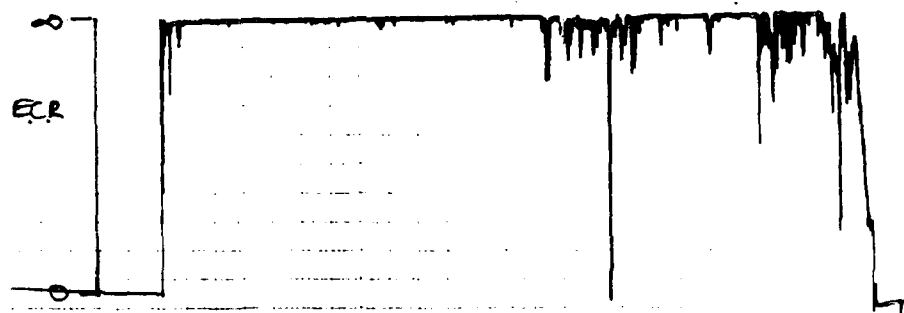
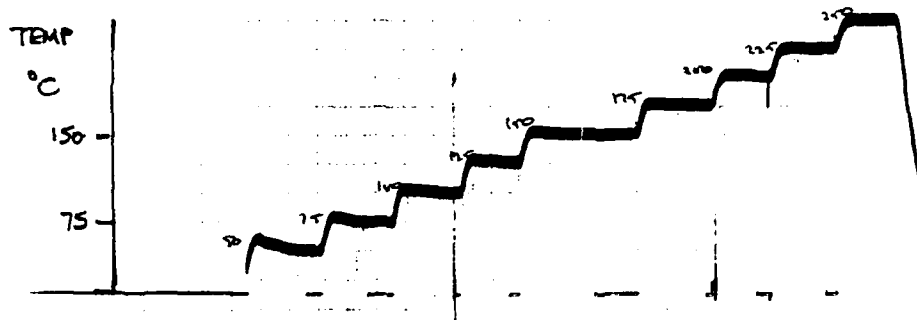
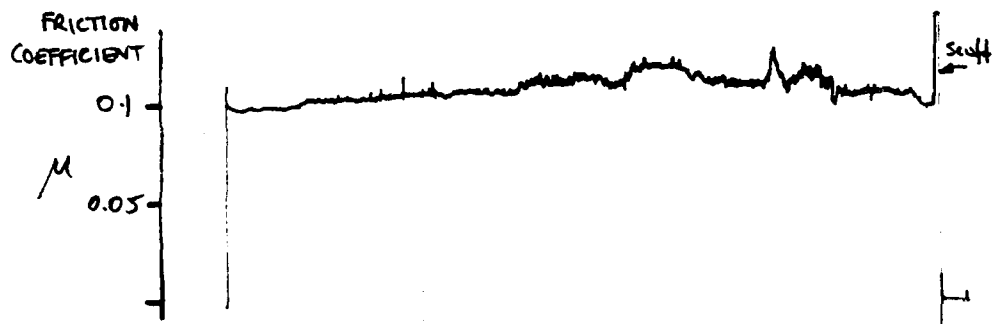


FIGURE 35

VARIATION OF FILM THICKNESS WITH TEMPERATURE  
 AT A CONSTANT LOAD OF 1 KG



500.SN + 19% PARALOX 15 BALL BEARING ON STEEL FLAT  
 ±0.5MM  
 34.5 Hz 1 kg LOAD

FIGURE 36

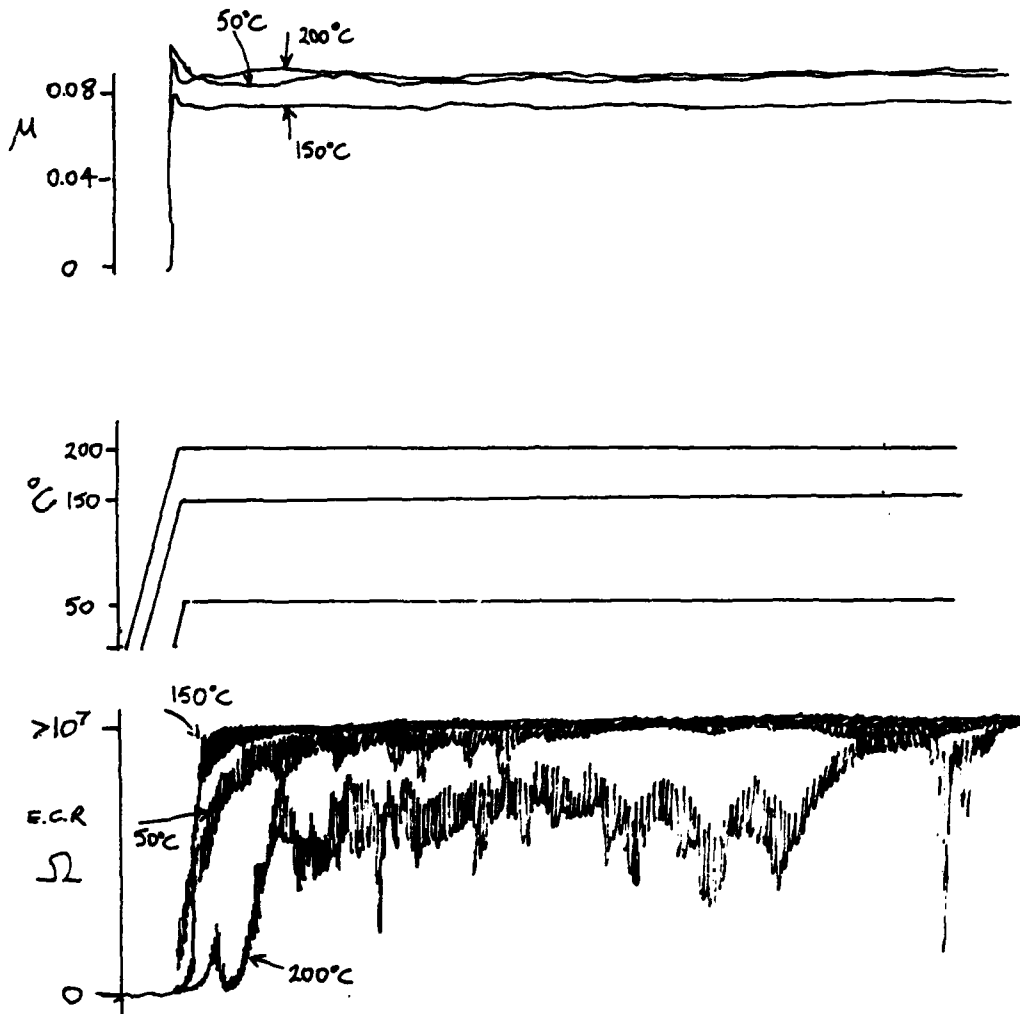


FIGURE 37

CAST IRON EXPERIMENTS AT DIFFERENT TEMPERATURES  
OIL A WITH 5 KG LOAD

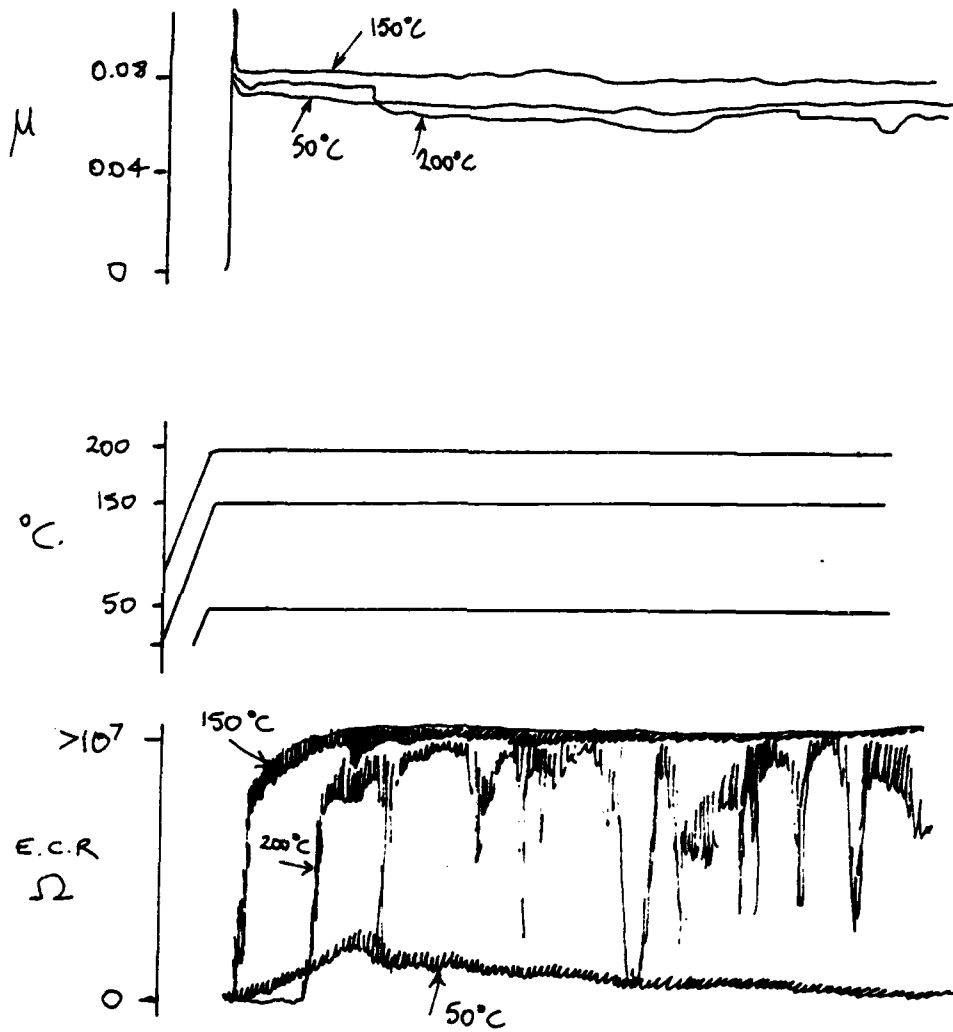


FIGURE 38

CAST IRON EXPERIMENTS AT DIFFERENT TEMPERATURES  
OIL B WITH 5 KG LOAD

APPENDIX

**A CORRELATION OF BENCH TESTS WITH ENGINES**

This phase of the work (detailed in Item 5 of the work statement C-1) can now begin, following the arrival of samples of engine parts and oils from Fort Belvoir.

It is proposed to investigate the running-in process in the various supplied cylinder liner/piston-ring pairs, together with oils from standard engine tests. The materials are detailed in Table 1 below, as supplied. The aim of this work is to try and gain a better understanding of what makes a 'good' surface. This will involve studying not only the run-in surfaces, but also the unworn surfaces, to see what features appear to make running-in and lubrication more favourable.

Table 1: Parts as supplied

Code	Engine	Oils (Ref. Nos.)
A	Caterpillar OL-5	AL-15930-L
B	Caterpillar OL-6	AL-15931-L
C	Caterpillar 1G2	AL-15932/33/34/35-L
D	Cummins NTC-400	AL-15936-L
E	John Deere 6404	AL-15937-L
F	Mack T-7	AL-15939-L

- 1 Experiments at first will be restricted to using cylinder liner/oil pairs with the reciprocating specimen being a ball, not a segment of piston-ring. This is for ease of use. Piston-ring segments are scheduled for a later stage.
- 2 A series of tests will be conducted on the running-in of each cylinder liner/oil pair, along the following lines, depending on experimental results

1  
2  
Run-in for 5 minutes at 150 - 350°C\* and constant load  $\frac{1}{5}$  kg.  
30  
120

Conditions of frequency and stroke amplitude will be typical of previous experiments, i.e. 35 Hz and  $\pm 0.5$  mm. Run-in will proceed in the series of temperatures until lubricant or surface failure is observed. This is detected by a rapid rise in the friction force.

The unworn and run-in surfaces will then be characterised by surface profilometry. Details about changes in various surface parameters - especially the mean curvatures of the asperities - will be recorded. Changes in these parameters can be correlated with observations of how the surfaces ran-in (e.g. the friction force variations; the rate of formation of the reaction film; the 'quality' of the reaction film when formed), as well as to visual, optical and scanning electron microscopic observation of the run-in surfaces.

- 3 In the case of liner C (see Table 1), where 4 oils are available, a matrix of tests can be performed to attempt to 'rank' the oils in order of 'best performance'. This ranking could be done on a criterion of the amount of wear that takes place, or possibly from the point of view of how various surface parameters are affected. Rankings will be obtained at different temperatures, to see if the lubricant performance changes according to this working condition.
- 4 In the light of the above experiments, a further range of experiments can be performed using alternative combinations of cylinder liner/oil, to determine how specific is the matching between oil and cylinder liner.

---

\*Temperature steps will at first be 25°C but may be increased to 50°C, depending on the observed sensitivity to temperature. Once more the uncertainty of the interfacial ring/liner temperature in running diesels makes itself felt.

It is hoped that these experiments and observations will substantially add to our understanding of exactly what makes a 'good' run-in surface. Also we hope to show that lubricants proved and ranked in engine tests can also be ranked in this laboratory test machine.

#### **B RHEOLOGY OF REACTION FILMS**

This work, which was started in the first year of the contract, will continue in tandem with the above tests. These experiments are at an advanced stage, and it is expected that a detailed set of results will be available for presentation at the Leeds/Lyon Symposium on Tribology in September 1987.

The shear strength of reaction films formed by ZDDP in a base oil in the reciprocating ball-on-flat contact are studied as a function of load, speed (or shear rate) and temperature. From this study, together with measurements of film thickness by capacitance, deductions can be made about the rheology of the reaction films. They are found to be low shear strength (1-10 MPa) solids, with shear behaviour similar to conventional polymers.

#### REFERENCES

- 1 KAPSA, Ph, MARTIN, J M, Boundary lubricant films: a review, Trib. Int., 1982, 15, 37-42
- 2 FUREY, M J, Film formation by an antiwear additive in an automotive engine, ASLE Trans., 1959, 2, 91-100
- 3 GEORGES, J M, MARTIN, J M, et al., Mechanism of boundary lubrication with zinc dithiophosphate, Wear, 1979, 53, 9-34
- 4 KASTING, G B, The composition of four-ball wear-scar films formed by crankcase lubricants, ASLE Trans., 1985, 28, 351-357
- 5 FUREY, M J, Metallic contact and friction between sliding surfaces, ASLE Trans., 1961, 4, 1-11
- 6 FIENNES, W G, ANDERSON, J C, An analysis of voltage discharge measurements in lubrication research, Proc. I. Mech. E., C112/72, 1972, 109-119
- 7 HIGGINSON, J G, The failure of elastohydrodynamic lubrication, PhD Thesis, Cambridge University, England, 1984
- 8 SAKAMOTO, T, UETZ, H, FÖHL, J, KHOSRAWI, M A, The reaction layer formed on steel by additives based on sulphur and phosphorus compounds under conditions of boundary lubrication, Wear, 1982, 77, 139-157
- 9 COY, R C, QUINN, T F J, An application of electron probe microanalysis and X-ray diffraction to the study of surfaces worn under extreme pressure lubrication, Proc. I. Mech. E., 1972, C94, 62-68
- 10 TONCK, A, MARTIN, J M, KAPSA, Ph, GEORGES, J M, Boundary lubrication with anti-wear additives: study of interface film formation by electrical contact resistance, Trib. Int., 1979, 12, 209-212
- 11 FOWLES, P E, JACKSON, A, MURPHY, W R, Lubricant chemistry in rolling contact fatigue - the performance and mechanism of one anti-fatigue additive, ASLE Trans, 1980, 24, 107-118
- 12 BOWDEN, F P, TABOR, D, The friction and lubrication of solids, in Int. Series of Monographs on Physics, Clarendon Press, Oxford, 1986
- 13 WINER, W O, in Appendix to CZICHOS, H, BECKER, S, LEXOW, J, Multilaboratory tribotesting: results from the Versailles advanced materials and standards programme on wear test methods, Wear, 1987, 114, 109-130
- 14 SNYDER, F L, TEVAARWERK, J L, SCHEY, J A, Effects of oil additives on lubricant film thickness and traction, SAE Paper No. 840263, 1984
- 15 JOHNSTON, G, CANN, P M E, SPIKES, H A, A new mechanism of gear and bearing anti-wear additive behaviour. 5th International Colloq. 'Additives for lubricants and operational fluids', Esslingen, 1986, Paper 3.12, 1-16

- 16 MILLS, T N, CAMERON, A, Basic studies on boundary, EP, and piston-ring lubrication using on special apparatus, ASLE Trans., 1981, 25, 117-124
- 17 ALLISTON-GREINER, A F, CAMERON, A, GREENWOOD, J A, Basic mechanisms of diesel lubrication correlation of bench end engine tests, 1st Interim Report, January 1986
- 18 ALLISTON-GREINER, A F, CAMERON, A, GREENWOOD, J A, Basic mechanisms of diesel lubrication, correlation of bench and engine tests, 2nd Interim Report, July 1986
- 19 BAILEY, M W, CAMERON, A, The effects of temperature and metal pairs on scuffing, ASLE Trans., 1972, 16, 121-131
- 20 LUNN, B, Epilamen und Mischreibung, ZVDI Berichte, 1957, 20, 41-46
- 21 HAMILTON, G M, MOORE, S L, The lubrication of piston rings, Proc. I. Mech. E., 1974, 188, 253-268
- 22 HAMILTON, G M, The hydrodynamics of cam follower, Trib. Int. 1990, 13, 113-119
- 23 GALVIN, G D, NAYLOR, H, WILSON, A R, The effects of pressure and temperature on some properties of fluids of importance in elasto-hydrodynamic lubrication, Proc. I. Mech. E., 1963, 178, 283-290
- 24 DYSON, A, NAYLOR, H, WILSON, A R, The measurement of oil-film thickness in EHD contacts, Proc. I. Mech. E., 1965, 180, 119-134
- 25 CANN, P M E, JOHNSTON, G J, SPIKES, H A, The formation of thick films by phosphorus-based anti-wear additives, Proc. I. Mech. E., Tribology - friction, lubrication and wear fifty years on, C208/87, 1987, 543-554
- 26 ROUNDS, F G, Additive interactions and their effect on the performance of a zinc dialkyldithiophosphate, ASLE Trans., 1977, 21, 91-101
- 27 BARCROFT, F T, PARK, D, Interactions on heated metal surfaces between zinc diathyldithiophosphates and other lubricating oil additives, Wear, 1986, 108, 213-234
- 28 MONTEIL, G, LONCHAMPT, J, ROQUES-CARMES, C, Study of anti-wear properties of zinc dialkyldithiophosphates through sliding-induced electronic emission, Proc. I. Mech. E., Tribology - friction, lubrication and wear - fifty years on, C224/87, 1987, 531-536
- 29 BRISCOE, B J, SCRUTON, B, WILLIS, F R, The shear strength of thin lubricant films, Proc. Roy. Soc. Lond., 1973, A333, 99-114
- 30 AMUZU, J K A, BRISCOE, B J, TABOR, D, Friction and shear strength of polymers, ASLE Trans., 1977, 20, 354-358

END

DATE  
FILMED

7 88